β-Bursts over Frontal Cortex Track the Surprise of Unexpected Events in Auditory, Visual, and Tactile Modalities

Joshua R. Tatz[1,2], Alec Mather[1], and Jan R. Wessel[1,2]

Abstract

■ One of the fundamental ways in which the brain regulates and monitors behavior is by making predictions about the sensory environment and adjusting behavior when those expectations are violated. As such, surprise is one of the fundamental computations performed by the human brain. In recent years, it has been well established that one key aspect by which behavior is adjusted during surprise is inhibitory control of the motor system. Moreover, because surprise automatically triggers inhibitory control without much proactive influence, it can provide unique insights into largely reactive control processes. Recent years have seen tremendous interest in burst-like β frequency events in the human (and nonhuman) local field potential—especially over (p)FC—as a potential signature of inhibitory control. To date, β-bursts have only been studied in paradigms involving a substantial amount of proactive control (such as the stop-signal task). Here, we used two cross-modal oddball tasks to investigate whether surprise processing is accompanied by increases in scalp-recorded β-bursts. Indeed, we found that unexpected events in all tested sensory domains (haptic, auditory, visual) were followed by low-latency increases in β-bursting over frontal cortex. Across experiments, β-burst rates were positively correlated with estimates of surprise derived from Shannon's information theory, a type of surprise that represents the degree to which a given stimulus violates prior expectations. As such, the current work clearly implicates frontal β-bursts as a signature of surprise processing. We discuss these findings in the context of common frameworks of inhibitory and cognitive control after unexpected events. ■

INTRODUCTION

Throughout the day, we constantly encounter external information translated by our various senses. While navigating this diverse sensory environment, our brain steadily generates predictions about this incoming stream of cross-modal information (Phillips et al., 2016; Egner, Monti, & Summerfield, 2010). One of the key roles of frontal cortex is to detect deviations from such sensory predictions (Kim, 2014; Corbetta & Shulman, 2002). Indeed, identifying and modifying behavior according to unexpected perceptual events can have profound consequences on our lives. For instance, seeing a predator, hearing a roar, or feeling something crawl on one's skin are all unexpected events that require rapid behavioral and cognitive adjustments. Subsequently, unexpected events provide a useful backdrop with which to explore the processes underlying adaptive behavior.

Indeed, unexpected perceptual events trigger multiple well-established cognitive and motor processes. Friston's (2010) influential free-energy principle suggests that descending neural volleys convey predictions about the sensory environment, whereas ascending volleys convey violations of these expectancies, or prediction error. Some work has used simple mathematical models (Baldi & Itti, 2010; Shannon, 1948) to quantify surprise at the single-trial level, thereby showing that various neural signals may reflect such straightforward computations (e.g., Nassar, Bruckner, & Frank, 2019; Wessel & Huber, 2019; O'Reilly et al., 2013; Mars et al., 2008). In addition to surprise processing, unexpected events are thought to capture attention in a bottom–up fashion and may interrupt goal-directed attentional representations, as in Corbetta and Shulman's (2002) "circuit breaker" model of attention. Along these lines, target detection ability (e.g., Asplund, Todd, Snyder, Gilbert, & Marois, 2010), attentional representations indexed by steady-state visual evoked potential (e.g., Soh & Wessel, 2021), and content in active working memory may all be impaired by unexpected events (e.g., Hakim, Feldmann-Wustefeld, Awh, & Vogel, 2021; Wessel, 2018a). Likewise, unexpected events prompt inhibition and disrupt ongoing action. Task-irrelevant unexpected events can induce RT slowing (e.g., Parmentier, Elford, Escera, Andrés, & San Miguel, 2008) as well as disrupt repetitive finger tapping (Horstmann, 2015) or the maintenance of isometric force contractions (Novembre et al., 2018). In addition, numerous studies using TMS to measure cortico-motor excitability have found a broad physiological suppression of the cortico-motor system after unexpected events, including at entirely task-irrelevant

[1]University of Iowa, [2]University of Iowa Hospital and Clinics

Journal of Cognitive Neuroscience 35:3, pp. 485–508
https://doi.org/10.1162/jocn_a_01958

muscles (Tatz, Soh, & Wessel, 2021; Iacullo, Diesburg, & Wessel, 2020; Dutra, Waller, & Wessel, 2018; Wessel & Aron, 2013).

Further underscoring the link between surprise and inhibitory control, unexpected events, and action cancellation are accompanied by common neurophysiological signatures. As the gold standard method of testing action cancellation, the stop-signal task (SST) is the primary tool used to study motor inhibition (Verbruggen et al., 2019). In the SST, prepotent responses to go signals must be inhibited upon interruption by an infrequent stop signal. One common signature that is observed both after such stop-signals and after unexpected events outside of stop-signal paradigms is the above-mentioned suppression of the motor system (Tatz et al., 2021; Wessel, Reynoso, & Aron, 2013; Cai, Oldenkamp, & Aron, 2012; Badry et al., 2009). Another common signature is the fronto-central (FC) P3 ERP. The FC P3 ERP accompanies unexpected events and stop signals and is likely generated by the same underlying neural generator (Wessel & Huber, 2019; Dutra et al., 2018). Furthermore, the frontal cortex regions of right inferior frontal cortex and pre-SMA that are reliably active during successful response inhibition are likewise active when inhibition is required and following unexpected events that do not instruct response inhibition (e.g., Sebastian et al., 2021; Levy & Wagner, 2011). Together, these findings provide evidence for common inhibitory processes that are active during both action stopping and surprise processing.

A missing link in this picture concerns the role of β-frequency burst events, which have attracted considerable recent attention as a newly discovered inhibitory signature in the local field potential. β-bursts are transient, nonlinear activity increases in β band activity (15–29 Hz) that occur in both cortical and subcortical regions of the brain (Diesburg, Greenlee, & Wessel, 2021; Tinkhauser et al., 2018; Feingold, Gibson, DePasquale, & Graybiel, 2015). β-bursts have been shown to represent time–frequency dynamics at the single-trial level more accurately and better predict behavior than average β power (Wessel, 2020; Little, Bonaiuto, Barnes, & Bestmann, 2019; Shin, Law, Tsutsui, Moore, & Jones, 2017) and are potentially generated by a straightforward biophysical mechanism that maps onto inhibitory and excitatory thalamocortical dynamics (Sherman et al., 2016). In line with their purported role in reflecting inhibitory neural processes, several studies have recently linked β-bursts to motor inhibition. Little and colleagues (2019) showed that sensorimotor β-bursts that occurred close to movement increased RT. Wessel (2020) demonstrated that healthy adults exhibit decreased bilateral sensorimotor β-bursts in the moments leading up to motor execution along with further decreases in contralateral sites just before movement. The same study and subsequent work have identified relationships between β-bursts at more frontal sites and action cancellation. Wessel (2020) found that successful stop trials were characterized by an increase in FC β-bursts, which in turn prompted increased β-bursting at the bilateral sensorimotor sites. Jana, Hannah, Muralidharan, and Aron (2020) similarly observed an increase in frontal β-bursts on successful stop trials and found that their latency correlated with the latency of the downturn of subthreshold electromyographic activity evoked on a portion of successful stop trials. Because these increases in β-bursts occurred at around 120 msec following the stop signal and precede global motor suppression-recorded TMS (~140 msec), Jana and colleagues (2020) suggested that these β-bursts may be a signature of the triggering of the stop process (see also Choo, Matzke, Bowren, Tranel, & Wessel, 2022). Diesburg and colleagues (2021) identified β-burst increases in local field potential recordings from subthalamic nucleus (STN) and motor thalamus on successful stop trials and further showed that these subcortical β-burst were associated with subsequent, low-latency sensorimotor β-bursts. Tinkhauser and colleagues (2018) found resting state phase coupling between STN and motor cortex that was increased during β-bursts. This suggests β-bursts may provide a vehicle of long-range communication during inhibitory motor control. Finally, β-bursts have been linked to pathophysiology of disease (Lofredi et al., 2019; Piña-Fuentes et al., 2019; Anidi et al., 2018), and clinical procedures aimed at targeting STN β-bursts in individuals with Parkinson's disease have shown promise in alleviating motor symptoms (Tinkhauser, Pogosyan, Little, et al., 2017; Tinkhauser, Pogosyan, Tan, et al., 2017).

Given the above-mentioned tight link between surprise and inhibition, and given the tight relationship between the novel β-burst signature and inhibitory control, one straightforward hypothesis is that β-bursts should be increased after unexpected events, even those that do not explicitly instruct the stopping of actions. Such a demonstration would be important for establishing a role of β-bursts in reactive inhibitory control. By reactive inhibitory control, we mean inhibition that is triggered by a stimulus rather than its anticipation (Aron, 2011). In the SST, the stop signal occurs on only a fraction of trials and uncertainty surrounds when it will occur. Consequently, some reactive inhibitory control is likely triggered by the stop signal. However, participants are not only aware that the stop signal will occur but are explicitly monitoring for it. Consequently, in the SST, reactive inhibitory control processes are necessarily conflated with proactive inhibitory control, or adjustments made in anticipation of the expected stop signal (Aron, 2011). Unexpected events offer a cleaner window into reactive control because such events prompt inhibition even when none is required by the task and, indeed, even when inhibition may be antithetical to task goals (Wessel, 2018a). In addition, nonselective corticospinal excitability suppression, which is a direct measurement of the physiological suppression of the motor system (Duque, Greenhouse, Labruna, & Ivry, 2017), is evident following unexpected events (Iacullo et al., 2020; Wessel et al., 2013). Such inhibitory control

signatures that are observed both during instructed action-stopping (such as in the SST) and after unexpected events likely reflect reactive inhibitory control (though of course they may be modulated by the presence of proactive control, e.g., in the SST).

The primary goal of the current study was hence to investigate whether frontal β-bursts, known to be found after stop-signals, are also elevated following unexpected events, indicating their role in reactive inhibitory control. To this end, we used two data sets. In the first data set, participants completed a trimodal cross-modal oddball (CMO) task in which unexpected events could occur randomly and without warning in auditory, visual, and haptic modalities. In the second data set, participants completed a bimodal CMO task in which unexpected events occurred in either the auditory or visual modalities. This second data set was previously reported by Wessel and Huber (2019) but is here newly analyzed for β-bursts. Regarding the first data set, we hypothesized that frontal β-bursts would be increased in all three modalities. The second data set then served as replication for the question of whether elevated β-bursts would be found following unexpected events. As additional research questions, we also examined the relationship of these β-bursts to surprise model estimates and RT at the single-trial level. To this end, we used the first data set exploratorily and the second data set (from Wessel & Huber, 2019) to independently verify (as initial confirmatory evidence) any exploratory findings generated from the first data set.

METHODS

Participants

Data Set 1 includes 40 healthy young adult volunteers (21 women; 5 left-handed; M_{age} = 21.35, SD = 4.17, range = 18 to 40 years). Data from three additional participants were excluded (two because of technical error in the CMO task and one who was unable to complete the CMO task). Data Set 2 includes the 55 healthy young adults from Wessel and Huber (2019). Participants in both data sets were recruited from the Iowa City community and from among University of Iowa students seeking research credit for psychology classes. Participants were compensated with course credit or at a rate of $15/hr. Both experiments were approved by the local institutional review board (#201511709).

Previous work on β-bursts from our group has shown that, in the SST, increased FC β-bursts for successful stop compared with matched go trials show a large effect size (dz = .8). Subsequently, as few as 23 participants would be sufficient to attain 95% power for detecting an effect of equal size at an alpha level of .05. However, greater power is often required to establish reliable brain–behavior relationships. Prior work from our group on proactive β-bursts evinced such relationships with a sample of 41 participants (Soh, Hynd, Rangel, & Wessel, 2021). We therefore targeted a similar sample size in Data Set 1.

Before experimentation, piloting was performed to determine whether the unexpected events induced startle responses. A small group of participants completed the task while surface electromyography (EMG) was recorded from bipolar electrodes placed on the sternocleidomastoid. The continuous EMG was monitored, and visually detectable EMG bursts were interpreted as startle response. An initial, higher intensity vibration was found to produce startle response. We therefore opted for a lower intensity vibration experimentally and verified in one additional participant (after the main experiment) that none of the unexpected events in the CMO task produced startle response. We then repeated the CMO task with the high-intensity vibration and verified that the high-intensity vibration did produce the startle response.

Materials

The methods used in Data Set 1 are the same as in Data Set 2 except where otherwise noted. The methods reported here are adapted from Wessel and Huber (2019). Stimuli for both experiments were delivered using Psychophysics Toolbox 3 (Brainard, 1997) on MATLAB 2015 (MathWorks, Inc.) on an IBM-compatible computer running Fedora Linux. Visual stimuli were presented on an ASUS VG278Q low-latency flat screen monitor (144 Hz), and auditory stimuli were played at conversational levels (~70 dB SPL) through speakers positioned on either side of the monitor. Tactile stimuli were delivered over custom-built response devices (Engineering Electronics Shop, University of Iowa) that interfaced with a Psychtoolbox-compatible data acquisition device (UBS-1208FS, Measurement Computing Corporation) to record button presses from the thumbs and vibrate motors at rates of 8300 rotations per minute. The response/vibration device was only used in Data Set 1. In Data Set 2 (and during the SST for participants in Data Set 1), participants made responses with each index finger on a QWERTY keyboard.

Procedure

A diagram of the CMO tasks used in each data set can be found in Figure 1. In Data Set 1, each trial started with a white fixation cross centered on a black background that was displayed for 500 msec. This was followed by the cue that was displayed for 200 msec. On 80% of trials, the cue was a standard event consisting of a green circle and a 600-Hz sine wave tone. On the remaining 20% of trials, 6.7% of trials featured unexpected visual events, 6.7% featured unexpected auditory events, and 6.7% featured unexpected haptic events. Thus, the unexpected events could occur in any (but not multiple) sensory domain(s). The specific trials on which unexpected events occurred were pseudorandomly determined separately for each participant. The only stipulations were that the first three trials were always standard trials, equal numbers of each type of unexpected event were presented within a given

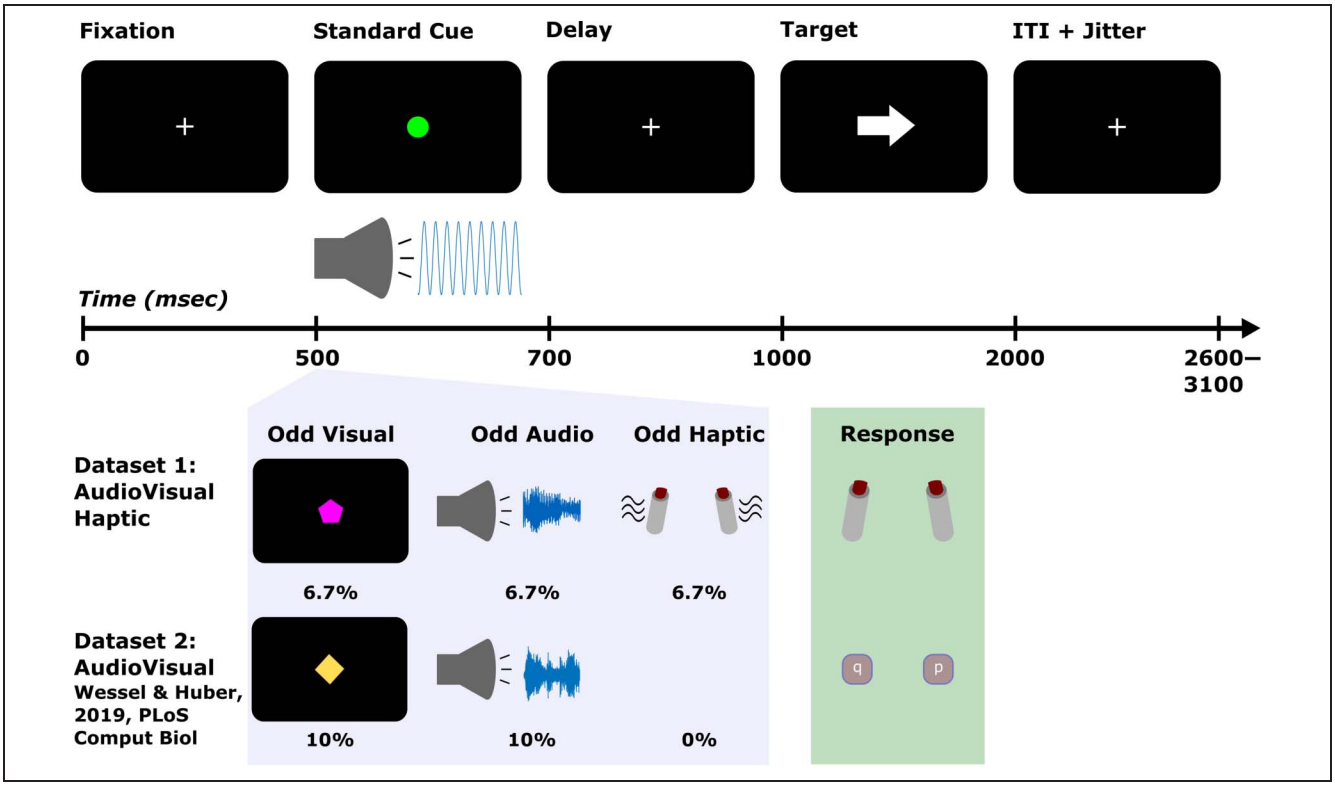

Figure 1. Task diagrams for the CMO tasks in Data Sets 1 and 2. The top row shows the timing and the display on standard cue trials (which were the same in both data sets). The standard cue consisted of a green circle and a 600-Hz pure tone. On trials with unexpected events, these were replaced by visual (unique shape/colors) or auditory novels (birdsong) or in the case of unexpected haptic events (in Data Set 1) the response devices participants held additionally vibrated. The light purple box illustrates examples of the unexpected events as well as their respective probabilities. The light green box depicts response devices (for Data Set 1, bilateral thumb presses, and for Data Set 2, bilateral index keypresses on a QWERTY keyboard).

block, and trials with unexpected events were always separated by at least one standard event trial. On unexpected visual trials, the green circle of the standard event was replaced by one of seven shapes (upward triangle, downward triangle, square, diamond, cross, hexagon, or serifed "I" shape) and one of 15 non-green colors equally spaced across the red, green, blue spectrum. Thus, the unexpected visual events were also unique or novel. Likewise, on unexpected auditory trials, the tone was replaced by a novel birdsong that matched the tone in amplitude. On unexpected haptic trials, the response devices that participants held in either hand vibrated bilaterally. The participants were instructed in advance about the properties of the standard event and that it was important to pay attention to this cue because it always took the same amount of time before the target would appear after the cue. Following presentation of the cue, the fixation was displayed for 300 msec before the presentation of the imperative stimuli. Thus, there was always a fixed delay of 500 msec before target onset. The target featured a left or right pointing arrow. The direction was pseudorandomly determined for each participant with the only stipulation that each trial type contained an equal number of left and right facing arrows within each block. Depending on the direction the target arrow pointed, participants pressed a button on the response/vibration device with the thumb of their corresponding hand. Participants were instructed to respond as quickly and accurately as possible and had to respond within 1000 msec following the presentation of the target. After the response deadline, a variable intertrial interval of 2600–3100 took place (in 100-msec steps, sampled from a uniform distribution) to preclude anticipation of the onset of the cue in the subsequent trial. Before beginning the formal experiment, participants completed 10 practice trials with no unexpected events. They then completed 240 trials in the main experiment, which were divided into four blocks of 60 trials with self-paced breaks in between.

The CMO task used in Data Set 2 was identical to Data Set 1 with two exceptions: In Data Set 2, 10% of trials featured unexpected auditory events and 10% featured unexpected visual events (thus, the overall frequency of the standard and unexpected events was kept the same across data sets 80%/20%). Participants also responded by pressing buttons on a QWERTY keyboard with their index fingers ("q" with the left index for left-pointing targets and "p" with the right index for right-pointing targets).

Following the CMO task, participants in both data sets completed the SST. The SST was included to verify that the same inhibitory signatures of interest (frontal β-bursts, FC P3) could also be identified following the stop signal. To this end, the SST was used as a functional localizer to identify whether the same electrodes captured β-burst differences across tasks and whether the FC P3 following unexpected events could be recovered from

an independent component reflecting the FC P3 following the stop signal (as in Wessel & Huber, 2019). As in Data Set 2, participants completed a standard visual SST consisting of 300 trials completed in six, 50 trial blocks. The stop-signal probability was .33 resulting in 200 go trials and 100 stop trials. The trial began with a black fixation cross presented for 500 msec on gray background. After this, the left- or right-pointing arrows (in black) were presented as the go signal. On go trials, participants pressed the "z" key on a QWERTY keyboard in response to left arrows and the "m" key in response to right arrows. On stop trials, the arrow turned red after the stop-signal delay (SSD) and participants were instructed to try their best to cancel their response while still responding as quickly and accurately as possible to the go signals. The SSD was initialized to 200 msec (separately for each hand) and increased in 50-msec increments following successful stop trials and decreased in 50 msec following failed stop trials. Trial duration was fixed at 3000 msec. Participants completed 24 practice (eight stop-signal) trials before the formal SST experiment began. One person followed instructions to respond as quickly as possible for the CMO task but did not do so for the SST (as evidenced by SSDs of 1000 msec indicating extreme waiting for the stop signal and nullifying the ability of the task to measure action cancellation). Data from this individual were only excluded from analyses involving the SST data.

EEG Recording

Scalp-surface EEG was acquired from a 62-channel passive electrode cap connected to BrainVision MRplus amplifiers (BrainProducts). Additional electrodes were placed over the left canthus of the left eye and beneath the left eye (on the orbital bone). The ground electrode was located at the Fz electrode position, and the reference electrode was placed at the Pz electrode. EEG was digitized at a sampling rate of 500 Hz.

EEG Preprocessing

Preprocessing was performed as described in Wessel and Huber (2019). We used custom MATLAB functions using the EEGLAB toolbox (Delorme & Makeig, 2004). The imported data were filtered with symmetric two-way least squares finite impulse response filters (high-pass cutoff: .3 Hz, low-pass cutoff: 30 Hz). Outlier statistics were used to automatically reject nonstereotyped artifacts (joint probability and joint kurtosis with cutoffs set to 5 *SD*s; cf. Delorme, Sejnowski, & Makeig, 2007). The data were rereferenced to the common average and subjected to temporal infomax independent component analysis (ICA) decomposition (Bell & Sejnowski, 1995) with extension to sub-Gaussian sources (Lee, Girolami, & Sejnowski, 1999). Among the resulting components, those corresponding to eye-movement and electrode artifacts were removed from the data based on outlier statistics and nondipolar components with residual variances greater than 15% (Delorme, Palmer, Onton, Oostenveld, & Makeig, 2012).

Behavioral Analysis

The RT data were initially submitted to a Bayesian repeated-measures (RM)-ANOVA with the factors Event Type (standard, unexpected audio, unexpected haptic, and unexpected visual) and Block (1, 2, 3, and 4) as within-subject factors. Moreover, as planned comparisons, Bayesian paired *t* tests were used to compare RTs following each type of unexpected event to those following the standard event within each block (for a total of 12 comparisons). Error rate and miss rate were similarly analyzed with Bayesian RM-ANOVAs and Bayesian paired tests. For these analyses and subsequent Bayesian tests, the data were analyzed using JASP 0.15.0.0 (Love et al., 2019) after exporting the data from MATLAB. Throughout, Bayes Factors (BFs) are framed as evidence favoring the alternative hypothesis (H1) or the null hypothesis (H0) with $BF \sim 1$ corresponding to inconclusive, $BF > 1$ corresponding to anecdotal evidence, $BF > 3$ corresponding to moderate evidence, and $BF > 10$ corresponding to strong evidence. For all tests, noninformative (or "empirical") priors are used.

The subsequent SST functional localizer task was examined in terms of the mean go-trial RT, mean failed-stop RT, and mean stop-signal RT (estimated via the integration method; Boehler, Schevernels, Hopf, Stoppel, & Krebs, 2014; Verbruggen & Logan, 2009).

Modeling Surprise at the Single-trial Level

There is some debate in the literature regarding the appropriate mathematical quantification of surprise (e.g., O'Reilly et al., 2013; Baldi & Itti, 2010; Shannon, 1948).

Based on Shannon's theory of information, surprise is given by the following equation:

$$\textit{Shannon Surprise}_i = -\log\left(p_{\textit{unexpected\_cue}}(1\ldots i-1)\right) \quad (1)$$

This equation quantifies the unexpectedness of the *i*th trial by taking the log inverse of the prior probability of the unexpected event. Because $-\log(0)$ is undefined, the surprise value for the first unexpected event (for which the prior is 0) was here defaulted to the next largest integer above the surprise value of the second unexpected event. The surprise values were different for each participant and computed independent of participant responses. Figure 2 provides an example of the Shannon surprise values from one participant from Data Set 1.

In contrast, Bayesian surprise (Baldi & Itti, 2010), an alternative quantification, uses the Kullback–Leibler divergence, and is given by the following equation:

$$\textit{Bayesian Surprise}_i = \log_2\left(\frac{p_{\textit{unexpected\_cue}}(1\ldots i)}{p_{\textit{unexpected\_cue}}(1\ldots i-1)}\right) \quad (2)$$

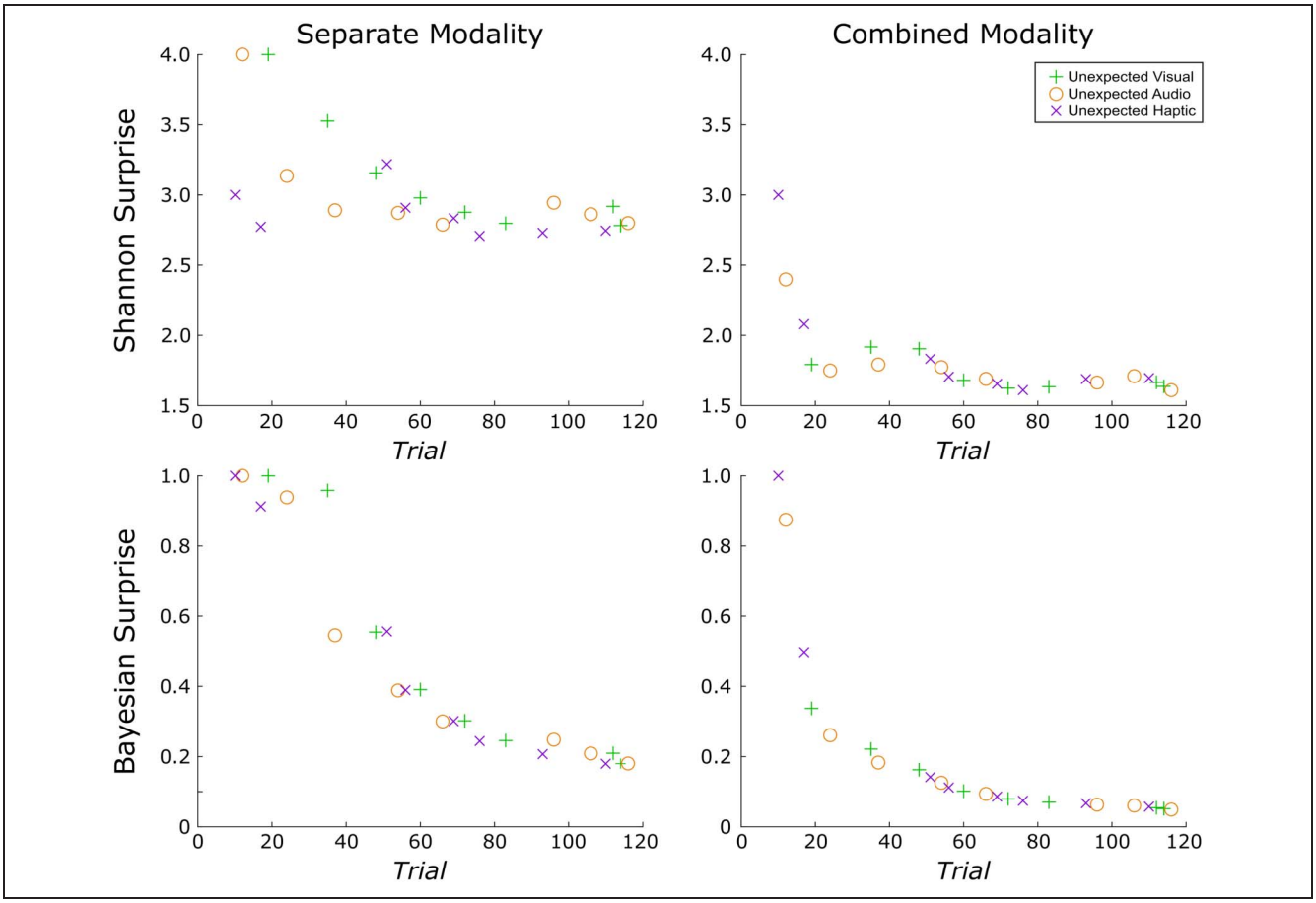

Figure 2. Example of the unique surprise model values from a single participant in Data Set 1. Surprise was quantified along two dimensions each with two levels. First, surprise was quantified according to each of two different formulas: (1) Shannon surprise, which is given by the inverse log of the probability of an unexpected event before its occurrence and (2) Bayesian surprise, which quantifies the difference in this probability and the updated probability after the unexpected event has occurred. Next, surprise was computed separately for each modality or combined (such that an unexpected haptic event is less surprising following an unexpected visual event). The ordering of trials containing unexpected events and thus the corresponding surprise values under each model varied across participants. Surprise values were computed independent of participant responses. Whereas the rate of decay is similar for combined modality models calculated using either surprise term, Shannon and Bayesian surprise differ somewhat when calculated separately for each modality. Namely, the decay is less rapid for Shannon surprise and is more affected by variations in the number of trials between successive unexpected events of the same variety.

Bayesian surprise captures the difference between the prior (denominator) and posterior probabilities of an event (numerator). For this reason, some have argued that Bayesian surprise should be more accurately termed "model updating" or "learning" (e.g., O'Reilly et al., 2013; Nassar et al., 2019). Here, the first surprising value following the first unexpected event was defaulted to 1 because $-\log(0)$ (and division by zero) is undefined.

Notably, both Shannon and Bayesian surprise contain the prior probability of an event and are therefore correlated (although they can be potentially disentangled through experimental instructions, as in O'Reilly et al., 2013). An important distinction, though, is that whereas Bayesian surprise considers the difference in prior and posterior expectations of a given stimulus (based on its relative likelihood before and after a given event), Shannon surprise provides a scaled version of the prior expectation alone and does not take the posterior expectation into account. This creates important conceptual distinctions between the different surprise models. Most notably, if a substantial number of standard trials occur before a given unexpected event, Shannon surprise can increase relative to the preceding unexpected event. By contrast, Bayesian surprise is always strictly monotonically decreasing. In the current CMO tasks, Shannon surprise better represents local deviations in the unexpectedness of events whereas Bayesian surprise represents learning the expected probabilities themselves (Wessel & Huber, 2019). It is also worth noting that some have argued that Shannon surprise relates more to reorienting attention and effecting rapid action adjustments whereas Bayesian surprise operates at a higher order and relates more to updating beliefs or internal models about the environment (O'Reilly et al., 2013).

Beyond the method for quantifying surprise (Shannon vs. Bayesian), in a data set that contains unexpected events originating in different modalities, a second question is whether surprise is modeled commonly across

modalities or for each modality separately (Wessel & Huber, 2019). This consideration has a substantial impact on the resulting surprise values. In the combined model, the surprise values decay even more rapidly as an unexpected event in the auditory modality is deemed less surprising even if it follows an unexpected event in the visual modality. Wessel and Huber (2019) modeled Bayesian surprise for both common and separate models and found that FC P3 amplitude was better predicted by the separate model, suggesting that frontal cortex separately accounts for these various sources of surprise. (For a replication and extension of this work with Data Set 1, please refer to the Appendix.) Of main interest, the present work provides a first examination of whether FC β-bursts relate to surprise. To this end, we again perform a model comparison that does not only compare Shannon versus Bayesian surprise, but also compares separate versus common surprise models across sensory modalities. Because the specific trials containing unexpected events and their ordering varied across participants, this also introduced variability in the corresponding surprise values under each model for each participant. Thus, any implicated surprise models in our single-trial model fitting analyses must be robust to this variability.

To complement the mean-based approach that examined RTs as function of event type and block (detailed in the previous subsection), we also fit surprise values to RTs at the single-trial level. To do so, standardized (z-scored) surprise values were regressed onto standardized (z-scored) RTs using robust regression [in MATLAB, *robustfit()*] to generate beta weights for each participant. Group-level inference was drawn on the resulting beta weights using Bayesian one-sample Wilcoxon-signed ranks tests to assess whether the surprise values reliably fit the data.

β-Burst Extraction

Before identifying β-bursts, we minimized the potential for volume conduction by transforming the data to a reference-free montage via the current source density method (Tenke & Kayser, 2005; Perrin, Pernier, Bertrand, & Echallier, 1989).

β-bursts were identified in the same manner as described by Shin and colleagues (2017) and Wessel (2020). The only exception is that we used a 2× median power threshold (in lieu of a 6× median power threshold) based on Enz, Ruddy, Rueda-Delgado, and Whelan's (2021) specification of optimal settings for β-burst detection. The description is adapted from Shin and colleagues (2017) as implemented in Wessel (2020):

First, each electrode's data were convolved with a complex Morlet wavelet of the form:

$$w(t,f) = A\exp\left(\frac{t^2}{2\sigma_t^2}\right)\exp(2i\pi ft) \qquad (3)$$

with $\sigma = \frac{m}{2\pi f}$, $A = \frac{1}{\sigma}\sqrt{2\pi}$, and $m = 7$ (cycles) for each of 15 evenly spaced frequencies spanning the β-band (15–29 Hz). Time–frequency power estimates were extracted by calculating the squared magnitude of the complex wavelet-convolved data. These power estimates were then epoched relative to the events in question (ranging from −500 to +2000 msec with respect to the cue in the CMO task, and − 500 to +1000 msec with respect to signal onset in the SST). Individual β-bursts were defined as local maxima in the trial-by-trial β-band time–frequency power matrix for which the power exceeded a set cutoff of 2× the median power (Enz et al., 2021) of the entire time–frequency epoch power matrix for that electrode (i.e., the median thresholding was performed across all epochs). Local maxima within each epoch were identified using the MATLAB function *imregionalmax()*.

β-Burst Analyses in the CMO Tasks

We focused on a FC region of interest for the β-burst analysis based on our previously reported finding involving a large SST data set (n = 234) showing maximal differences in beta burst rate in these electrodes on successful stop compared with match go trials (Wessel, 2020). To examine whether FC β-bursts were elevated following unexpected events and to potentially gain a better understanding of the time course of the β-bursts, we adopted a sliding window approach in place of the bin-based approaches used in prior work (e.g., Wessel, 2020). For this, we cycled through each sample beginning −100 msec before the onset of the cue and +500 msec after its onset and counted the number of bursts occurring within ±25 msec of the sample (with one sample corresponding to 2 msec of data). We then converted to burst rate by summing the number of bursts across trials and dividing by the number of trials. This process was completed for each of the FC electrodes of interest (FC1, FCz, FC2, C1, Cz, and C2). After this, we used the baseline period (−100 to 0 msec) to calculate the percent change in burst rate and to convert to percent change from baseline for each electrode. The resulting values were averaged across the FC electrodes. For these and all subsequent analyses, standard event trials that were immediately preceded by unexpected event trials were excluded. The data were then compared across each event type (standard, unexpected audio, unexpected visual, unexpected haptic). First, we used frequentist one-way RM-ANOVAs over each time point comparing percent change in burst rate across the various event types. Then, we used frequentist paired-samples t tests to compare each unexpected event type to the standard event. The initial, predefined alpha level of .05 was used for these tests. The alpha level was then adjusted for multiple comparisons via the false discovery rate (FDR) procedure (Benjamini, Krieger, & Yekutieli, 2006) correcting for the number

of tests (one for the ANOVA, three for the paired *t* tests in Data Set 1, and two for the paired *t* tests in Data Set 2) and the number of timepoints (250).

Next, the relationship between β-burst rate and surprise was explored. In each data set, we looked at the association between the number of β-bursts and surprise values on (nonrejected) trials containing unexpected events. In our initial, exploratory analysis with Data Set 1, we considered two different time ranges. First, we considered beta-bursts within the full cue-to-target interval (0 to +500 msec). As these results were exploratory and did not yield positive findings, we do not consider them further. Second, and after having established that, in line with our main hypothesis, FC beta-bursts were elevated following unexpected events in Data Set 1, we explored these relationships within a specific time window containing the elevated β-bursts. For this, we extracted the number of β-bursts between +75 and + 200 msec following each unexpected event. Both the number of bursts within these search windows and the surprise values (again for each type of surprise and for separate and combined modality considerations) were standardized as *z*-scores and a beta weight was computed using robust regression (with the *robustfit()* function in MATLAB) for each participant. To draw inferences at the group-level, the resulting individual beta weights were compared against zero using Bayesian one-sample Wilcoxon signed-ranks tests. We consider here the results of Data Set 1 to be purely exploratory, whereas we consider any potentially replicated results in Data Set 2 to provide initial, confirmatory evidence.

We then examined the relationship between RTs and β-bursts in each data set using similar single-trial level approaches. First, we considered whether the number of β-bursts predicted RT by computing Spearman rank correlations for each participant following unexpected events. For these analyses, we considered the specific time range (+75 to +200 msec following the event) and the full cue-to-target interval (0 to +500 msec) in both data sets. We then considered whether the latency of the β-burst in relation to the target was predictive of RT. As one approach, we extracted the latency of the β-burst that was nearest to the target (in the −250 to +250 msec surrounding the target) and again computed Spearman rank correlations for each participant. As another approach, we compared RTs across trials that contained β-bursts in the FCz electrode (which was selected as a representative electrode based on results from the main analyses) in the first half of the cue-to-target interval, the second half, both, and neither.

β-Burst Analysis in the SST

Lastly, we examined the dynamics of FC β-bursts in the SST (combined across Data Sets 1 and 2) using the sliding window approach from the CMO task to compare β-bursts on successful stop trials to matched go trials as well as to failed stop trials.

RESULTS

Behavior

The RT results of Data Set 1 closely matched those previously reported for Data Set 2 (Wessel & Huber, 2019) in all respects. The Bayesian RM-ANOVA on Event Type (standard, unexpected audio, unexpected visual, unexpected haptic) and Block (1, 2, 3, 4) indicated strong evidence for main effects of Event Type ($BF_{10} = 8.02 \times 10^4$) and of Block ($BF_{10} = 2.71 \times 10^9$). Strong evidence was also indicated for the Event Type × Block interaction over a model with only the two main effects ($BF_{10} = 268.1$). Most importantly, the basic comparisons between each type of unexpected event and standard events echoed the finding that all types of unexpected events induce RT slowing, but that—consistent with the notion of surprise adaptation—these differences wane over time. This was apparent as unexpected visual and unexpected auditory events both showed strong evidence of slowing compared with standard events in the first block (unexpected audio: $BF_{10} = 53.6$; unexpected visual: $BF_{10} = 2.12 \times 10^5$). Likewise, we found that unexpected haptic events also showed this slowing in the first block ($BF_{10} = 5.72$). Only anecdotal evidence was found for RT slowing following unexpected visual events in Block 2 ($BF_{10} = 1.10$) and Block 3 ($BF_{10} = 2.64$). None of the other unexpected events in Block 2 and onward showed evidence of RT slowing ($BFs_{01} > 1$). Thereby, the behavioral RT results replicated Wessel and Huber (2019) and extended them to the haptic domain (Figure 3).

The single-trial fits of RT and surprise lent themselves to similar conclusions as the mean-based approach to RTs, with some additional insights. There was strong evidence to suggest that Shannon surprise with separate modality terms positively predicted RTs ($BF_{10} = 20.49$), whereas there was moderate evidence against Shannon surprise with common modality terms predicting the data ($BF_{01} = 4.48$). Similarly, there was strong evidence that Bayesian surprise with separate modality terms positively predicted RTs ($BF_{10} = 24.26$), but only anecdotal evidence to suggest this for Bayesian surprise with common modality terms ($BF_{10} = 2.18$). Thus, participants' RTs appeared to follow both types of surprise, provided their values represented surprise separately for each type of unexpected event.

For mean error rates, there was a main effect of Event Type on error rate (strong evidence, $BF_{10} = 12.69$) but not of Block (strong evidence, $BF_{01} = 10.99$), nor was there an Event Type × Block interaction (strong evidence, $BF_{01} = 45.5$). The mean percent error rates for each event type were as follows: standard: 1.97%, unexpected auditory: 0.16%, unexpected visual: 1.09%, and unexpected haptic: 1.41%. Follow-up *t* tests on event type indicated that the main effect was driven by the lower number of errors following unexpected auditory events compared with standard events ($BF_{10} = 9.76 \times 10^5$). The evidence did not suggest that the other types of unexpected events differed from the standard (unexpected visual: $BF_{01} = 2.42$, unexpected haptic:

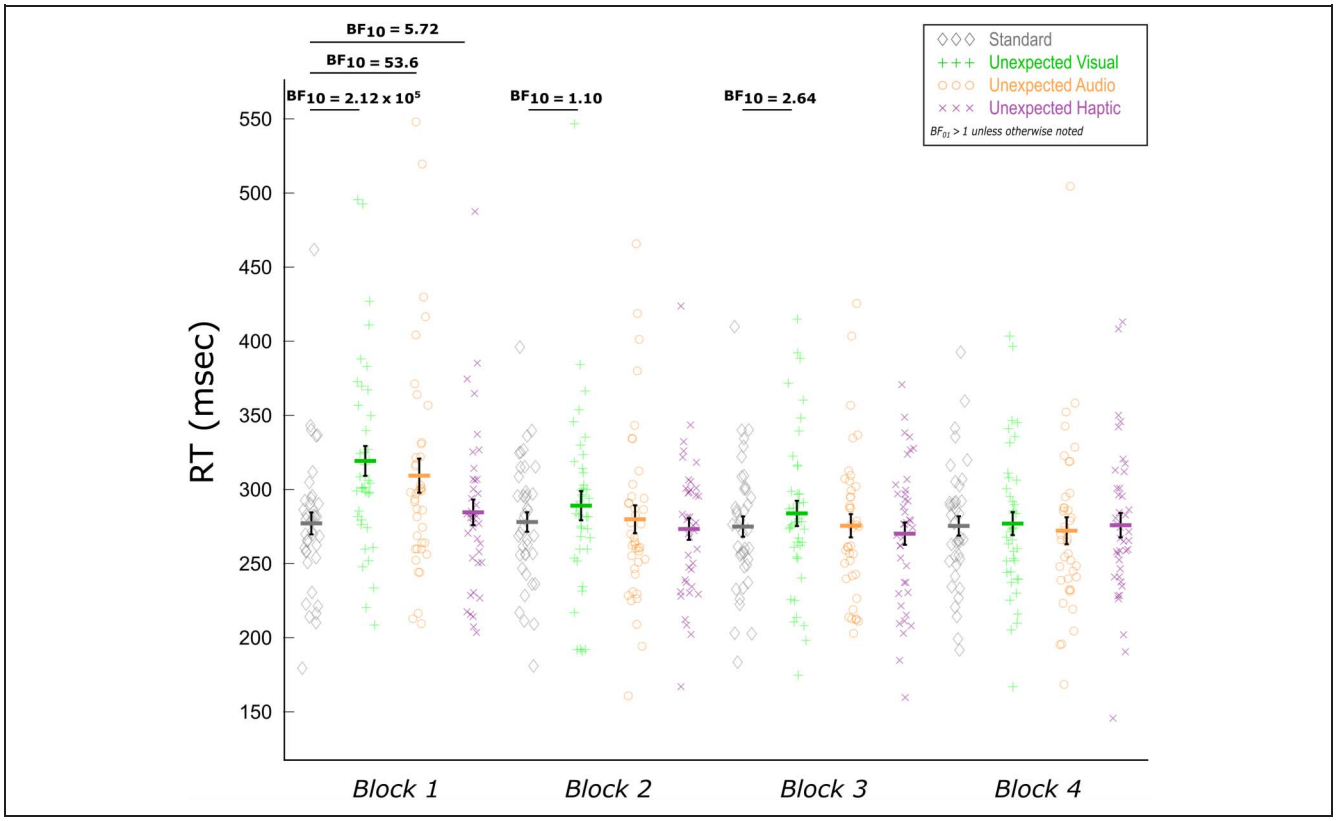

Figure 3. Mean RTs as a function of event type and block for the trimodal CMO task of Data Set 1. Paired Bayesian *t* tests indicated RT slowing following all three types of unexpected events in the first block. Consistent with the notion of surprise, these differences quickly dissipated as suggested by the lack of (or at least attenuated) differences in subsequent blocks. Black error bars indicate *SEM*.

BF_{01} = 6.17), nor did they differ from the unexpected auditory event (unexpected visual: BF_{01} = 1.22, unexpected haptic: BF_{01} = 9.90). This outcome contrasts those for Data Set 2, which showed increased error rates following unexpected auditory and visual events that remained stable across blocks. However, error and miss trials were generally rare and not considered in the EEG analyses.

For mean miss rates, the results were in line with the null findings of Data Set 2. Strong evidence was found for a lack of differences regarding event type (BF_{01} = 125.0), block (BF_{01} = 11.23), and the Event Type × Block interaction (BF_{01} = 311.6).

The SST also closely followed those from Data Set 2. Mean go RT = 535 msec, mean failed stop RT = 464 msec, mean stop-signal RT (SSRT, calculated via the integration method; Verbruggen et al., 2019) = 252 msec, and mean p(inhibit) = .52 (compared with Data Set 2: mean go RT = 520 msec, mean failed stop RT = 444 msec, mean SSRT = 252.00, and p(inhibit) = .51).

EEG

FC β-Bursts Are Increased following Unexpected Events in All Three Modalities

In Data Set 1, significantly increased β-bursting followed each type of unexpected event (see Figure 4). The one-way RM-ANOVAs did not return significant differences after FDR-correction (sustained differences at $p < .05$ were found from 78 to 138 msec and at 212 msec without correction). However, more importantly, comparing the sliding window trace for each unexpected event to the standard revealed significant β-burst increases following unexpected auditory events from 102 to 148 msec, following unexpected visual events from 116 to 118 msec, and following unexpected haptic events from 52 to 130 msec.

As can be seen in Figure 4, the unexpected haptic events appeared to prompt more robust increases in β-bursts than unexpected events in the other sensory modalities. It is important to note, though, that differences other than the modalities in question could account for these differences particularly because the unexpected haptic events always featured the same stimulus (rather than a novel) and because no haptic event was a part of the standard cue. Presumably, the lack of novelty among unexpected haptic events might have rendered them less unexpected whereas only encountering a haptic event on unexpected haptic event trials might have rendered such events more unexpected. Of course, we also cannot discount the possibility that fundamental differences between sensory modalities might also account for differences in β-burst characteristics following unexpected

events. For instance, β power appears to underlie communication between parallel sensorimotor representations of somatosensory and motor cortex (Baker, 2007) and sensorimotor β-bursts have been shown to play an important role in somatosensory perception (Law et al., 2022; Shin et al., 2017). Thus, β-bursts may be particularly important in the haptic domain. At present, we refrain from drawing comparisons across different types of unexpected events and instead focus on FC β-bursts that were common across different unexpected events and may thus reflect domain-general control mechanisms.

In Data Set 2, the RM-ANOVA detected significant differences across conditions from 110–232 msec (see Figure 5). These sliding windows coincided virtually identically with those identified for the unexpected auditory events compared with the standard event (106–232 msec). Although unlike in Data Set 1, we did not find significant increases following unexpected visual events by themselves, this was a consequence of the FDR correction. Without it (i.e., using $p < .05$), β-bursts were again increased following unexpected visual events (12–50 msec). This deviation from Data Set 1 notwithstanding, the overall results strongly suggest that, as predicted, β-bursts are generally increased following unexpected events.

As an alternative approach suggested to us by an anonymous reviewer, we repeated the above approach but, instead of using the prespecified FC ROI, we used a cluster of frontal electrodes that was identified based on the corresponding SST that participants completed after the CMO task in each data set. Specifically, we identified a group of contiguous frontal electrodes displaying significant ($p < .001$) increases in β-bursts for at least 10 consecutive time windows on successful stop compared with go trials in the pre-SSRT period. Of the electrode clusters meeting these criteria, we selected the one showing the maximal difference. For Data Set 1, this cluster consisted of electrodes FCz, FC1, Cz, and C1. This analysis yielded highly similar results to the original analysis. Significant (FDR-corrected according to the original analysis) β-burst increases were found following unexpected auditory events from 100 to 150 msec; unexpected haptic events from 90–124, 128–132 msec; and unexpected visual events at 98, 102–112, and 116–118 msec. For Data Set 2, a cluster of electrodes consisting of FC1, FCz, FC2, C1, AF4, FC4, F2, F4, and F6 were identified as reflecting heightened β-bursts on successful stop compared with go trials. Significant β-burst increases were found following unexpected auditory events from 52–56 msec, 106–244 msec, and 254–272 msec; as well as following unexpected visual

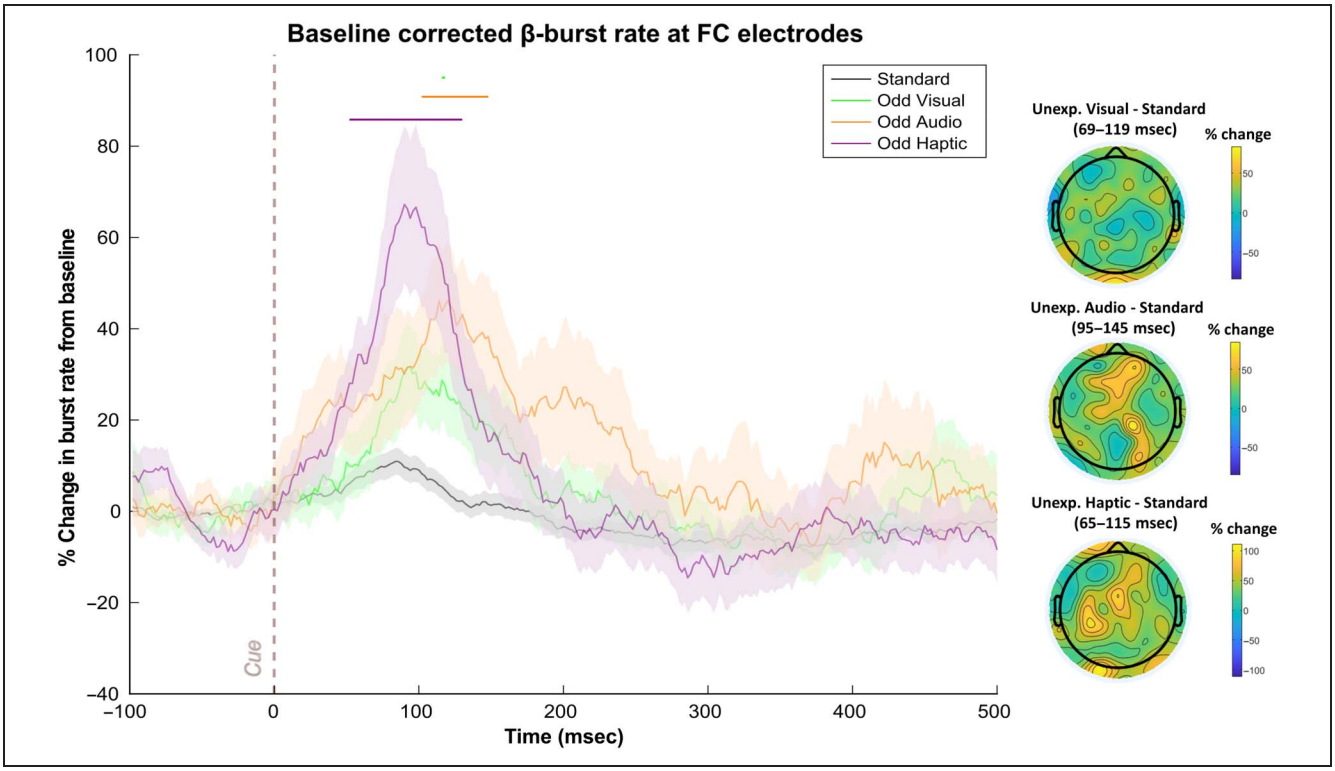

Figure 4. FC β-bursts following unexpected events in Data Set 1 ($n = 40$). (Left) Depicts the percent change in β-burst rate relative to baseline for ±25-msec sliding windows calculated for each 2-msec timepoint. An increase in β-bursts at FC sites was evident following unexpected events in all three modalities at early latencies. Sliding window timepoints with significant differences (FDR-corrected, $p = .05$) across event types are denoted by horizontal lines at the top of the plot (black: RM-ANOVAs across all event types, green: unexpected visual vs. standard, orange: unexpected auditory vs. standard; purple: unexpected haptic vs. standard). Shaded regions indicate *SEM*. (Right) Scalp topography differences depicting the % change in β-bursts at all electrodes in the ±25-msec window surrounding the maxima for each unexpected event type identified with the sliding window technique relative to the same time period for the standard event.

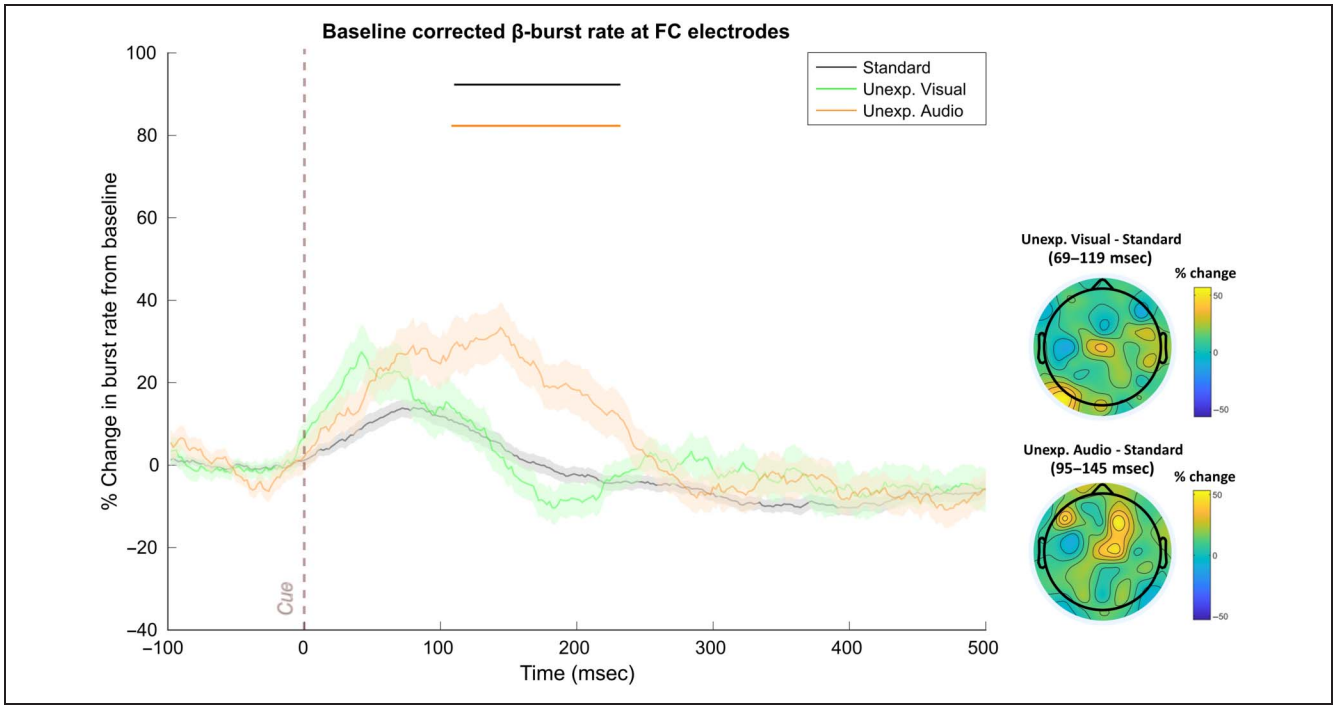

Figure 5. FC β-bursts following unexpected events in Data Set 2 (n = 55). (Left) Depicts the percent change in β-burst rate relative to baseline for ±25-msec sliding windows calculated for each 2-msec timepoint. An increase in β-bursts at FC sites was evident following unexpected auditory events. The numerical increase in β-burst rate following unexpected visual events did not achieve significance. Sliding window timepoints with significant differences (FDR-corrected, p = .05) across event types are denoted by horizontal lines at the top of the plot (black: RM-ANOVAs across all event types, green: unexpected visual vs. standard, orange: unexpected auditory vs. standard). Shaded regions indicate *SEM*. (Right) Scalp topography differences depicting the percent change in β-bursts at all electrodes in the ±25-msec window surrounding the maxima for each unexpected event type identified with the sliding window technique relative to the same time period for the standard.

events from 58–62 msec and at 364 msec. These analyses thus complemented the original analyses in implicating early latency increases in β-burst rate following each type of unexpected event.

Early FC β-Bursts Reflect Modality-specific Shannon Surprise Terms

We used Data Set 1 for exploratory analyses of potential relationships between FC β-bursts and surprise. We then aimed to replicate any such findings using Data Set 2. After having identified that FC β-bursts were increased following unexpected events in Data Set 1, we considered these relationships within a specific time range that contained the period during which unexpected events were followed by significant increases in β-bursts (75–200 msec after event onset). The individual-subject beta weights from these analyses are plotted in Figure 6A. Shannon surprise with separate modality terms for each modality was positively associated with β-bursting as *BF* indicated moderate evidence that the mean beta weight at the group level was above zero (BF_{10} = 7.20). Contrastingly, *BF*s for the other surprise models indicated moderate evidence for no relationship (Shannon surprise/combined terms: BF_{01} = 5.81, Bayesian surprise/separate terms: BF_{01} = 3.82, Bayesian surprise/combined terms: BF_{01} = 2.40).

To confirm these exploratory findings, we completed the same analyses using Data Set 2. The individual-subject beta weights are plotted in Figure 6B. Just as in Data Set 1, there was moderate evidence that Shannon surprise with separate model terms positively predicted FC β-bursting (BF_{10} = 3.58). Although there was again moderate evidence for no relationship regarding Shannon surprise with combined modality terms (BF_{01} = 6.54), this time, there was anecdotal evidence suggesting positive relationships for Bayesian surprise with separate terms (BF_{10} = 2.53) and Bayesian surprise with combined terms (BF_{10} = 1.29). Here, it may be worth mentioning that in the trimodal data set, any given unexpected event was less frequent than in the bimodal data set. Consequently, the difference between Shannon surprise and Bayesian surprise values should be relatively more pronounced in Data Set 1 owing to the longer stretches of trials between successive unexpected events of the same ilk. This could potentially explain why Bayesian surprise models appeared to show some hint of a relationship in Data Set 2 that was not observed in Data Set 1. Either way, Shannon surprise with modality-specific terms consistently outperforms the other models across both data sets.

We next sought to corroborate these findings using the ROIs based on the frontal electrodes showing increased β-bursts on successful stop trials in the SST participants completed after their respective CMO tasks. The specific

electrodes used for each data set in these analyses are detailed in the previous section. For Data Set 1, there was strong evidence (BF_{10} = 400.01) indicating that Shannon surprise with separate modality terms positively predicted β-bursts. For the other surprise models, anecdotal to moderate evidence was provided against an association between surprise values and β-bursts (Shannon surprise/common modality: BF_{01} = 5.81, Bayesian surprise/separate modality: BF_{01} = 2.02, Bayesian surprise/common modality: BF_{01} = 1.64). For Data Set 2, there was again strong evidence (BF_{10} = 35.01) indicating a positive association between Shannon surprise with separate modality terms and β-bursts. As with the original ROI, there was moderate evidence against an association for Shannon surprise with common modality terms (BF_{01} = 3.16), anecdotal evidence for an association with Bayesian surprise with separate modality terms (BF_{10} = 1.42), and anecdotal evidence for an association with Bayesian surprise with common modality terms (BF_{10} = 2.35). Thus, these results also clearly establish a relationship between β-bursts and Shannon surprise with separate modality terms, although here, the β-bursts may bear a tighter connection to action stopping given that these participants showed increased β-bursting in the same electrodes during successful stopping in the SST.

No Observed Relationships between FC β-Bursts and RT in the CMO Task

We next investigated relationships between RT and FC β-bursts. No reliable associations were found between the number of FC β-bursts and RTs on unexpected event trials in either data set with either time range (Data Set 1, full-time range: BF_{01} = 5.62, constrained time range: BF_{01} = 2.67; Data Set 2, full-time range: BF_{01} = 5.41, constrained time range: BF_{01} = 6.67). Neither were reliable associations found on standard event trials (Data Set 1, full-time range: BF_{01} = 5.29, constrained time range: BF_{01} = 5.68; Data Set 2, full-time range: BF_{01} = 6.76, constrained time range: BF_{01} = 4.02). We also did not observe evidence for relationships between the latency of β-bursts in the −250 to +250 msec surrounding the onset of the target and RT (Data Set 1: unexpected events: BF_{01} = 4.85, standard events: BF_{01} = 4.74; Data Set 2: unexpected events: BF_{01} = 4.83, standard events: BF_{01} = 6.06). Finally, we compared RTs on trials depending on whether β-bursts in the FCz electrode (as a representative electrode across all ROIs) were found in the first half of the cue-to-target interval, the second half, both, or neither. Bayesian RM-ANOVAs did not indicate any differences among these conditions (Data Set 1: BF_{01} = 16.13; Data Set 2: BF_{10} =

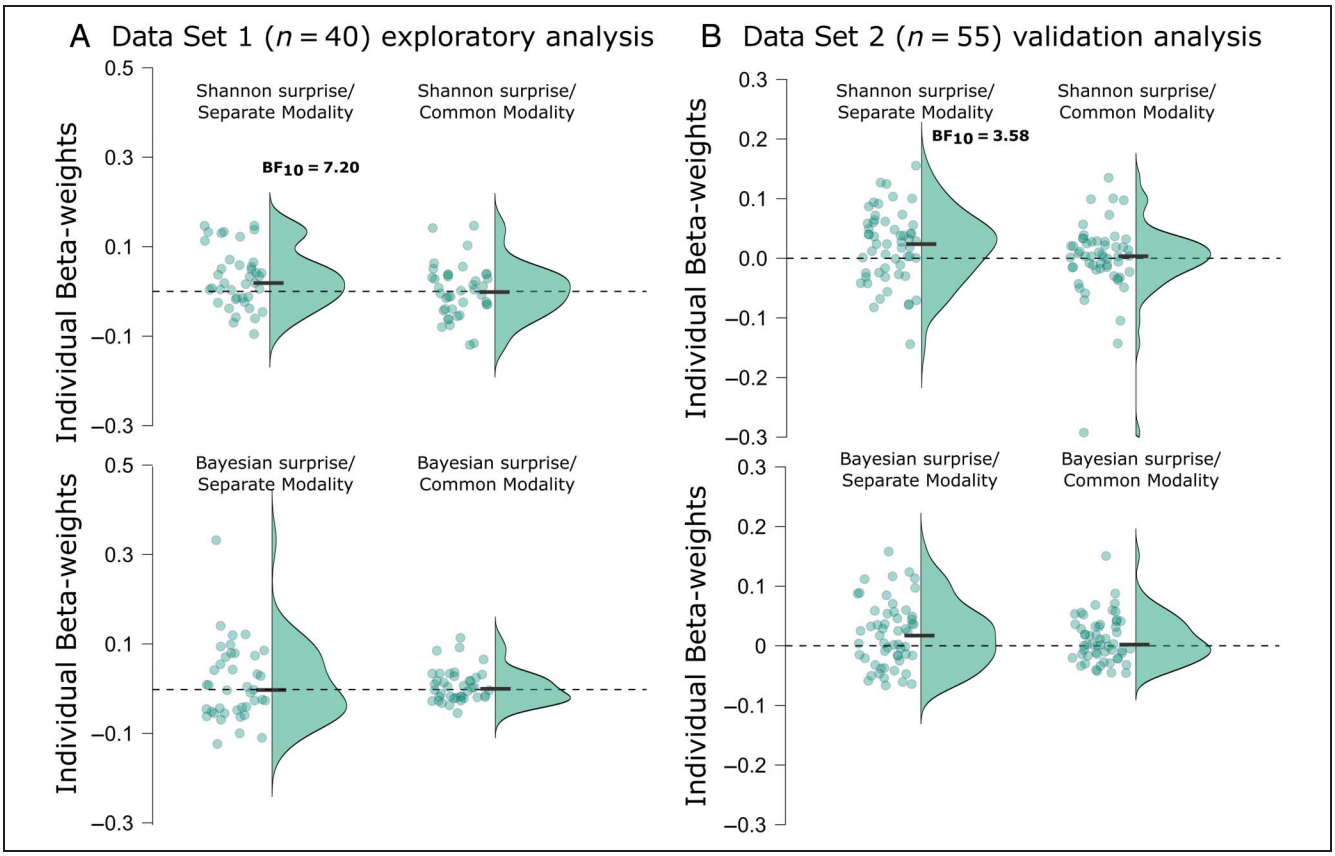

Figure 6. Individual beta weights from the various *z*-scored surprise single-trial model values fitted to *z*-scored β-bursts from 75 to 200 msec following unexpected events. (A) Points represent mean beta weights from individual participants estimated via robust regression for each surprise model in Data Set 1. Half violin plots depict the distribution of beta weights. Black bars indicate mean beta weights. (B) The same as in A but for Data Set 2, which was used to validate potential findings in Data Set 1. Reported BF_{10}s correspond to moderate evidence in favor of the alternative hypothesis. BF_{10}s < 3 are not shown here (but are reported in the main text).

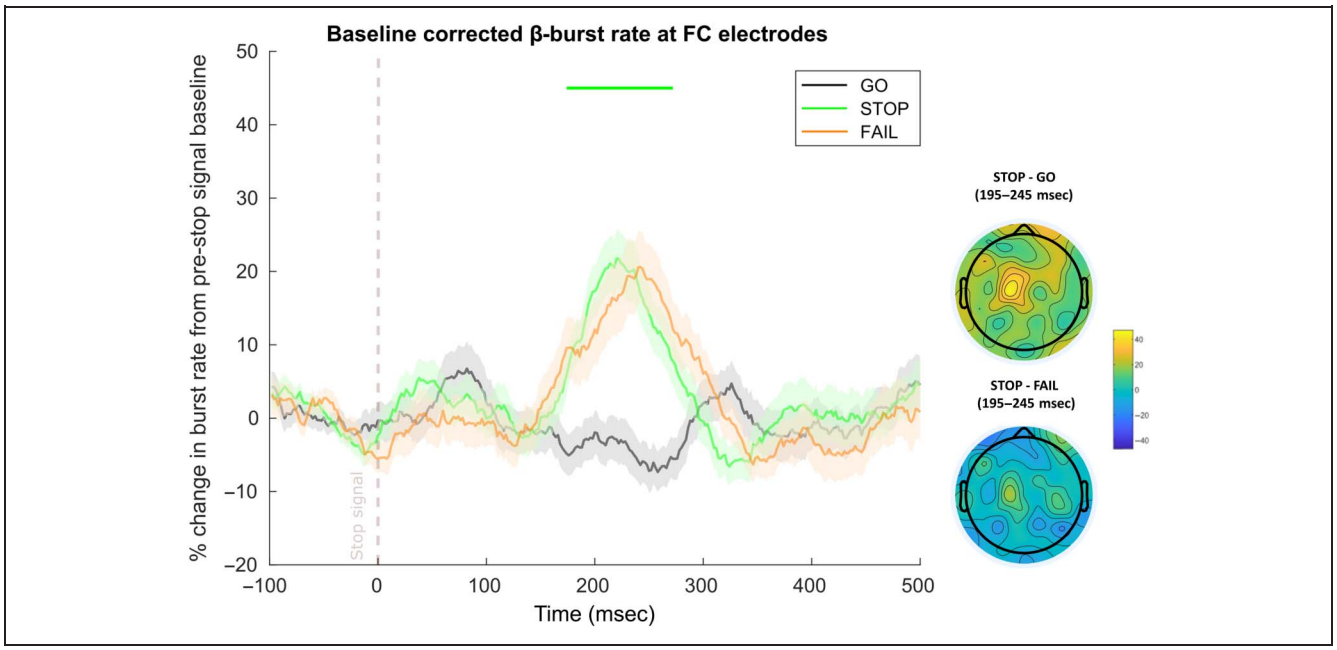

Figure 7. FC β-bursts following the stop signal in the SST (n = 94, combined from Data Sets 1 and 2). Depicts the percent change in β-burst rate relative to baseline for ±25-msec sliding windows calculated for each 2-msec timepoint. β-bursts at FC sites were increased on successful stop trials (stop) compared with matched go (go). Failed stop trials (fail) did not differ from successful stop trials. Sliding window timepoints with significant differences (after FDR correction) across trial types are denoted by horizontal lines at the top of the plot (green: successful stop vs. matched go). Shaded regions indicate *SEM*. (Lower right) Scalp topography differences depicting the percent change in β-bursts at all electrodes in the ±25-msec window surrounding the maximum for successful stop compared with matched timepoints on go and failed-stop trials.

1.27). In the Discussion section, we discuss potential reasons for the present lack of relationships between β-bursts and RT.

FC β-Bursts Are Increased after the Stop Signal

As can be seen in Figure 7, FC β-bursts were also increased following the stop signal. In the SST (from Data Sets 1 and 2, n = 94), FC β-bursts were increased on successful stop trials compared with matched go trials from 174 to 272 msec. This replicates prior work documenting increased β-bursting at frontal sites following the stop signal (Jana et al., 2020; Wessel, 2020). Interestingly, no time point differences were found for successful compared with failed stop trials. However, the peak burst rate latency for successful stops appeared to precede that for failed stops (Figure 7). This parallels the main finding involving FC P3 in which the amplitude peaks earlier on successful stop trials (e.g., Kok, Ramautar, De Ruiter, Band, & Ridderinkhof, 2004) and would suggest that the process related to FC β-bursts begins (or at least comes to fruition) sooner on these trials.

Timing Differences of FC β-Bursts and FC P3 following Unexpected Events in the CMO Task and the Stop Signal in the SST

Figure 8 depicts the differences in FC β-burst rate following each type of unexpected event and the standard in the CMO task of Data Set 1 as well as the difference between successful stop and matched go trials in the corresponding SST. It is interesting that the time range of increased FC β-bursts following the stop signal appeared to occur later than the time ranges in which we found increased FC β-bursting following unexpected events in the CMO task. Similarly, an examination of the activity corresponding to the FC P3 as captured by the IC that best reflected the stop signal P3 (i.e., that showed a maximum difference in activity at frontal sites and highest correlation to the original channel space ERP; Wessel & Huber, 2019) suggested that the P3 process appears to begin sooner following unexpected events in the CMO task than on successful stop trials in the SST. Finally, the FC β-burst peaks in each condition and task also appeared to precede the earliest differences in the corresponding FC P3 (as isolated with the IC that best reflected each participant's stop signal P3).

Following a suggestion from an anonymous reviewer, we completed an exploratory analysis to assess for statistical differences in these latencies at the individual-subject level. To examine latency differences in β-bursts, we used the sliding window approach for each participant to extract the peak burst rate within +50 to +400 msec following each type of unexpected event in the CMO task and following the stop signal on successful stop trials in the SST. To identify P3 onset, we first identified the maximum difference in the stop signal IC in each participant during the same time range (although P3 is typically extracted with a later time range, here it was important to search within the same time range). We then used permutation

testing (with Markov Chain Monte Carlo simulations) on each time point moving backward from the maximum difference to identify the earliest timepoint that showed a statistically significant difference ($p < .05$) with consecutive significant timepoints leading up to the maximum difference (Wessel & Huber, 2019; Wessel & Aron, 2015).[1]

Bayesian Wilcoxon signed-ranks tests indicated moderate evidence that the peak burst latency following unexpected haptic events in the CMO task occurred earlier than after the stop signal on successful stop trials in the SST ($BF_{10} = 6.26$). However, despite numerically earlier peak burst latencies, there was moderate evidence for no difference between unexpected auditory events and the stop signal ($BF_{01} = 4.84$) and anecdotal evidence for no difference between unexpected visual events and the stop signal ($BF_{01} = 1.77$). In Data Set 2, strong evidence indicated that the peak burst latencies following both unexpected auditory and unexpected visual events preceded the peak burst latency for the stop signal (unexpected auditory: $BF_{10} = 1.48 \times 10^4$, unexpected visual: 19.81). Strong evidence indicated that the onset of the FC P3 (isolated from the stop signal IC) following each type of unexpected event occurred earlier than that for the stop signal (Data Set 1, unexpected auditory: $BF_{10} = 204.19$; unexpected visual: $BF_{10} = 273.86$, unexpected haptic: $BF_{10} = 36.56$; Data Set 2, unexpected auditory: $BF_{10} = 133.14$; unexpected visual: $BF_{10} = 6423.26$). In the Discussion section, we speculate on the possibility that inhibitory processes may be accelerated following unexpected events in settings that do explicitly require inhibition.

When comparing the peak burst latencies to the FC P3 onsets, strong evidence indicated that the peak burst latency following unexpected haptic events preceded the corresponding onset of the FC P3 ($BF_{10} = 673.10$), but such evidence was lacking for the other types of unexpected events (unexpected auditory: $BF_{01} = 1.93$, unexpected visual: $BF_{01} = 5.12$). In the SST, the peak burst latency on successful stop trials also preceded the

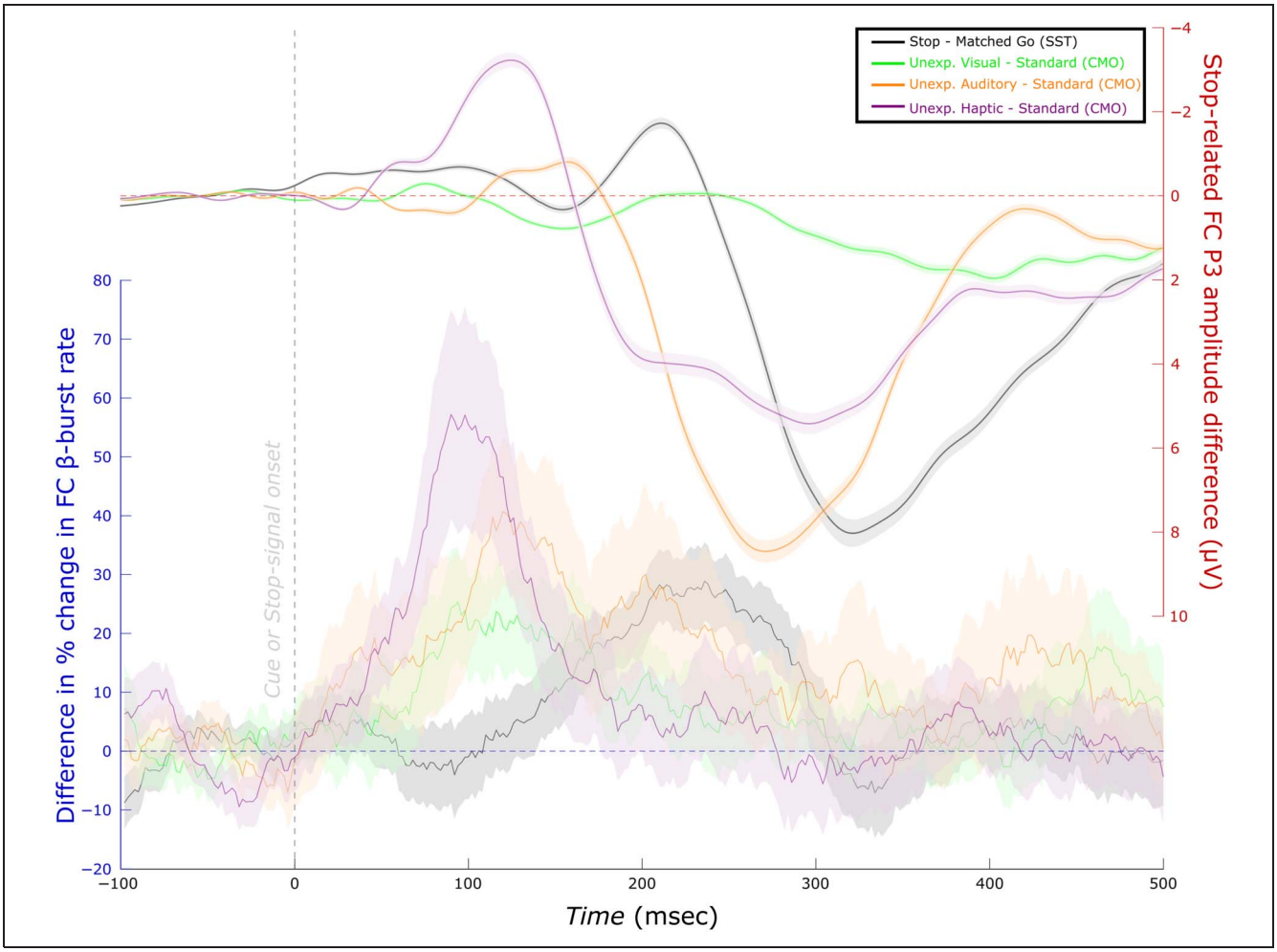

Figure 8. Time-course of differences in FC β-burst rate compared with FC P3 (Data Set 1, $n = 39$). (Left scale) Differences in the percent change in β-burst rate for successful stop trials compared with matched go trials (from Figure 7, but only involving Data Set 1 participants) as well as unexpected events relative to standard (from Figure 4). (Right scale) The same differences for FC P3. For this, the SST was used as a functional localizer to isolate an IC corresponding to the FC stop-signal P3 in the merged data set (i.e., the CMO and SST in Data Set 1). Visual inspection indicates that FC β-burst differences precede the corresponding FC P3 differences. Unexpected event differences generally also precede stop differences (excepting the FC P3 for unexpected visual events).

corresponding P3 onset (BF_{10} = 7.15). In Data Set 2, the peak burst latency following unexpected auditory events preceded the corresponding P3 (BF_{10} = 1.58 × 10^5), although moderate evidence was found for no difference for unexpected visual events (BF_{01} = 5.10). Once again, the peak burst latency on successful stop trials preceded the corresponding P3 onset (BF_{10} = 3.06). Overall, these findings provide some support for the notion that FC β-bursts precede the FC P3. This was most apparent within the SST. It bears mentioning that these tests may have been conservative for potential timing differences given that peak burst latency was compared with a measure of the onset of the FC P3. Nevertheless, the combined evidence across tasks and data sets suggest that FC β-bursts reflect an earlier occurring signature than the FC P3.

DISCUSSION

We found clear and consistent support for our prediction that FC β-bursts would be increased following unexpected events. In Data Set 1, which included unexpected events in auditory, visual, and haptic modalities, increased β-bursting at frontal electrode sites was evident in all three modalities. In Data Set 2 (from Wessel & Huber, 2019), which included unexpected events in the auditory and visual modalities, increased FC β-bursting was evident following unexpected auditory events and, numerically, following unexpected visual events. To our knowledge, this represents the first investigation of β-bursts following unexpected events.

Jones and colleagues have recently suggested a role for β-bursts in the detection of sensory events. In particular, Shin and colleagues (2017) showed that β-bursts over somatosensory cortices originating 300–100 msec before tactile stimulus delivery impaired perception whereas Law and colleagues (2022) showed that β-bursts contemporaneous with stimulus delivery aided perception. Although we did not explicitly explore the consequences of β-bursts on perception, our results suggest that FC β-bursts may also play a role in stimulus detection and perhaps in registering their surprise value. The finding of early increased FC β-bursting following unexpected events compared with standard events already suggests that these bursts may play a role in the detection of infrequent events. However, our finding that these bursts also scale with Shannon surprise on just the subset of trials with unexpected events joins and expands upon this finding to suggest that this infrequency-representation happens at very fine-grained scale (capturing trial-to-trial deviations in expected probabilities).

Across both data sets, FC β-bursting was linked to a specific type of surprise: Shannon surprise with separate terms for each modality. Although correlated, Shannon surprise and Bayesian surprise differ mainly in that an unexpected event can have a higher surprise value than its predecessor with a sufficiently long stretch of intermediate expected events according to the Shannon model. Our experimental design did not explicitly attempt to dissociate the two types of surprise (which has been previously attempted, e.g., in O'Reilly et al., 2013). Given that Bayesian surprise and Shannon surprise were correlated in the data sets, however, it is even more interesting that FC β-bursts specifically correlated with Shannon surprise in both cases, and to a consistently lesser extent with Bayesian surprise. It is unlikely that this dissociation is explainable in terms of differing degrees of sensitivity to detect either relationship as both types of surprise were predictive of RT and the whole-brain EEG data corresponding to the FC P3 response at the single-trial level (for analyses relating FC P3 to surprise, see Appendix). Prior work has indicated that Shannon surprise and Bayesian surprise relate to at least somewhat distinct neural processes. For instance, using fMRI, O'Reilly and colleagues (2013) identified activity within posterior parietal cortex as representing Shannon surprise whereas activity in anterior cingulate cortex and pre-SMA uniquely represented Bayesian surprise (i.e., updating, as they refer to it). Scalp-surface EEG studies suggest that whereas FC P3 better characterizes Bayesian surprise, Shannon surprise is better characterized by centro-parietal P3 (Wessel & Huber, 2019; Seer, Lange, Boos, Dengler, & Kopp, 2016; Kolossa, Kopp, & Fingscheidt, 2015; Mars et al., 2008). Interestingly, the present results suggest that FC β-bursts might represent a unique frontal cortex neural correlate of Shannon surprise and one that emerges sooner than the P3 components. To our knowledge, this represents the first demonstration of a signature of Shannon surprise over frontal cortex. Presumably, this early detection of infrequent events or surprise could serve to pave the way for rapid adjustments to behavior and cognition (Diesburg & Wessel, 2021; Wessel & Aron, 2017; O'Reilly et al., 2013).

The time course of this increase in FC β-bursts and its relation to surprise was further interesting. Although the sliding window approach we employed to analyze β-bursts still introduces temporal uncertainty as to the precise timing with which increased β-bursting begins, we could at least be confident that FC β-bursts were elevated soon after the presentation of the unexpected event and well before 200 msec. This is important in establishing FC β-bursts as a potentially early signature because, notably, the putative onset of the FC P3 process within the context of action stopping occurs subsequently, around 200 msec (Wessel & Aron, 2015). At the group level, increases in FC β-bursting appeared to occur well before the onset of the FC P3 in both the CMO task and the SST (see Figure 8). By adopting an individual subject-level approach to comparing peak burst latency and FC P3 onset, we were further able to show that peak β-bursting following unexpected haptic events in Data Set 1 and unexpected auditory events in Data Set 2 preceded the onset of the corresponding P3. Although we did not find evidence for differences with the other unexpected events, it is worth noting that comparing the peak of the β-burst process to the onset of

the P3 may be quite conservative. Moreover, peak β-bursting following the stop signal preceded the onset of the corresponding P3 in both data sets. These findings offer some initial insight into the potential processes that the FC β-burst signature might relate to within a couple of our theoretical frameworks. Wessel and Aron's (2017) adaptive re-orienting theory of attention and Diesburg and Wessel's pause-then-cancel model (2021, see also: Schmidt & Berke, 2017) commonly propose multistage models whereby an early stage is characterized by global inhibition of the motor system brought about by the detection of unexpected or otherwise salient, behaviorally relevant events, which is then followed by a later stage in which more strategic adjustments and updates to ongoing motor and cognitive programs occur. Based on the timing of various functional neurophysiological signatures and their relation to behavior, Diesburg and Wessel (2021) have proposed certain functional signatures to be associated with either the purported early or late inhibitory stages. For instance, studies involving single-pulse TMS stimulation of M1 regions responsible for muscles irrelevant to the task at hand both within action stopping contexts (i.e., the SST or its variants) and following unexpected events have estimated global inhibition to begin around 150 msec, thus providing the main functional signature of the pause phase. Other signatures such as brief decreases in EMG around this time (Tatz et al., 2021; Jana et al., 2020; Raud et al., 2020; Raud & Huster, 2017) or the still earlier, transitory decreases in isometric force contractions (Novembre et al., 2018) also likely relate to this stage. By contrast, the main purported neurophysiological correlate of the cancel phase is the FC P3 signature, which has been tied to successful response inhibition in the SST and RT slowing following unexpected events. However, a direct neural correlate of the pause phase with precise timing such as EEG or magnetoencephalography is lacking. Moreover, based on previously observed timings of increased frontal β-bursting following the stop signal (Jana et al., 2020; Wessel, 2020), it remained unclear which processing stage this inhibitory signature related to and whether the increases in frontal β-bursting index reactive inhibitory control or might instead relate to proactive inhibitory control. In the primarily reactive context of the CMO task, elevated FC β-bursts emerged soon after event onset and would overall seem better aligned with the timing of the pause phase than the cancel phase. In the SST involving the same individuals, elevated β-bursting emerged somewhat later (~178 msec) but still before 200 msec and the emergence of the stop-signal P3. This timing is rather intermediate to the ~120-msec timing found by Jana and colleagues (2020) and the ~200-msec timing found by Wessel (2020), but nevertheless shifts the evidence in favor of a timing more consistent with the pause phase.

We also found that when isolating the FC P3 from the stop signal IC, the onsets of the FC P3 occurred earlier following each type of unexpected event in the CMO task than following the stop signal on successful stop trials in the SST. We also found peak β-burst latencies to occur earlier following unexpected haptic events than on successful stop trials in Data Set 1. We did not find earlier burst latencies following unexpected auditory or visual events in Data Set 1; however, we did in Data Set 2. Thus, an intriguing possibility is whether surprise accelerates the inhibitory process. Some initial evidence for this comes from Iacullo and colleagues (2020) who examined cortical-spinal excitability while participants responded to imperative stimuli that were quickly followed by standard tones, infrequent/expected tones, or novel/unexpected sounds. Critically, they found global motor suppression to occur earlier following novel/unexpected sounds compared with infrequent/expected tones. In contrast to surprising events, the SST contains not just the reactive inhibitory control brought about by the infrequent stop-signal itself, but also proactive inhibitory control, or strategic adjustments in anticipation of the stop-signal (Wessel, 2018b; Elchlepp, Lavric, Chambers, & Verbruggen, 2016). To better capture proactive control, researchers have created variants of the SST that include certain go trials (in contrast to the default, maybe stop trials). However, fMRI studies that have done so have implicated BOLD responses in the same regions (Jahfari, Stinear, Claffey, Verbruggen, & Aron, 2010; Chikazoe et al., 2009), and EEG studies have likewise implicated some of the same ERPs, including FC P3, in both types of control (Raud & Huster, 2017; Elchlepp et al., 2016). Soh and colleagues (2021) found increased sensorimotor β-bursts on maybe stop compared with certain go trials, a difference that was present even before trial onset. Interestingly, Muralidharan, Aron, and Schmidt's (2022) recent work modeling frontal β-bursts in the SST suggested that these bursts increased the decisional threshold necessary for the go response. Taken together, studies on the SST suggest that some of the same processes subserve proactive and reactive inhibitory control. If so, it would seem plausible that these processes might take place more rapidly when proactive control is minimal, as in the case of surprising events. From the standpoint of rapidly allocating resources and adjusting behavior, this would indeed be an adaptive feature as, at least in most real-world settings, the optimal course of action (or inaction) cannot be known in advance of the surprising event but instead must be urgently gleaned after its occurrence. For example, after detecting something suddenly crawling across their skin, one might decide to hold still. Unexpected events may therefore provide a framework that is better aligned with how inhibition transpires in our day to day (Wessel, 2018a). Overall, the current results are consistent with the notion that inhibitory processes may be accelerated with surprise. We note, though, that although all unexpected events prompted earlier FC P3 onset latencies compared with those evoked by the stop signal, the results concerning FC β-bursts were more mixed (i.e., with three of the five unexpected event conditions showing earlier latencies than on successful

stop trials). Most basically, we herein demonstrate that frontal β-bursts occur in reactive contexts.

In the present task designs, FC β-bursts were not directly related to the observed motor slowing. One possibility is that β-bursts reflect an early processing stage that only indirectly relates to RT. Within the proposed pause phase (Diesburg & Wessel, 2021), information must pass through cortex and multiple subcortical structures before arriving at primary motor cortex. By contrast, the proposed cancel phase is argued to more directly relate to actual behavioral adjustments. Subsequently, the correspondence of FC β-bursts with RT may have been too subtle to detect a relationship (even as RT is a highly variable measure itself), although this lack of relationship could still be consistent with pause phase roles of salient event detection or otherwise triggering inhibition. In addition, the FC P3, which is a prominent signature of the cancel phase, exhibited correspondences with RT following each type of unexpected event (see Figure A2). Another reason for not finding a connection between FC β-bursts and RT could owe to the nature and timing of our CMO task. In our task, unexpected events occurred as a part of a cue that occurred 500 msec before the imperative stimulus. Thus, any early inhibition prompted by the unexpected events might have been overcome by the time the stimulus appeared. Rather, the timing of our task may have been more optimal for capturing the impact of the cancel phase on inhibition, and indeed, we found relationships between RT and FC P3. In hindsight, the timing of increased FC β-bursting might have also occurred too soon. For instance, Little and colleagues (2019) showed that movement was only disrupted by sensorimotor β-bursts that occurred just before the response. Here, responses occurred even sometime after target onset (as participants completed a choice RT task). Given that these issues could have compounded in the present task design, it is interesting to consider whether a relationship between β-bursts and behavior might be established in a task in which unexpected events occur during movement, which could be assessed for instance by presenting unexpected events just after the first increase in electromyographic activity. Regardless, if global inhibition serves to promote rapid action adjustments in the first place, it would seem plausible that this process might be more active when actions are already underway.

In summary, we have shown that unexpected events in three modalities (auditory, haptic, and visual) prompt increases in FC β-burst rate soon after their onset and before 200 msec. These β-bursts further appear to track the surprise (or trial-to-trial fluctuations in stimulus infrequency) of these events separately for each modality and as indexed by Shannon surprise. Although we were unable to establish a relationship between FC β-bursts and RT, the overall results suggest that FC β-bursts may play an early role in inhibitory processes such as salient event detection and/or the triggering of the global inhibition characteristic of the pause phase.

APPENDIX

As a subsidiary goal of this study, we sought to identify whether the EEG data in Data Set 1 replicated the whole-brain event-related EEG findings reported by Wessel and Huber (2019), especially because their data were re-analyzed as Data Set 2. We also aimed to extend their findings to unexpected events originating from the haptic modality. In general, the results closely followed those of Wessel and Huber (2019), further underscoring the similarity of Data Sets 1 and 2, despite the inclusion of the third haptic modality in Data Set 1.

EEG Analyses following Wessel and Huber (2019)

We considered four results from Wessel and Huber (2019) to be of primary importance in replicating their work:

1) Single-trial EEG data should favor a model with separate Bayesian surprise terms in all three modalities (auditory, visual, and haptic).
2) Mean RT should be predicted by FC P3 in each modality.
3) The FC P3 following unexpected events should be recoverable from a FC IC isolated from the SST when used as a functional localizer (i.e., the stop-related FC P3).
4) The separate Bayesian surprise model should be implicated with this IC alone.

Given that we examined β-bursts for both Shannon and Bayesian surprise, for the sake of thoroughness, we also newly examined the above-mentioned analyses in Data Set 2 based on Shannon surprise. The ensuing description of the methods relevant to this subsection is adapted from Wessel and Huber (2019):

First, the surprise values originating from both types of surprise (Shannon, Bayesian surprise) and modality considerations (separate, combined) were used to model the whole-brain event-related single-trial EEG response on trials with unexpected events. We based this analysis on procedures reported by Fischer and Ullsperger (2013). To compare surprise models, at the single-trial level, we used robust regression [in MATLAB, *robustfit()*] to fit the standardized (*z*-scored) EEG signal with the standardized (*z*-scored) surprise values in each participant in each electrode in each trial in 48-msec time windows spanning from 50 to 500 msec. These data were baseline corrected with the data from −100 to 0 msec and averaged across trials (48 trials, barring those excluded because of artifacts). For each model specification, this resulted in a 64 (channel) × 10 (time point) = 640 matrix of beta weights. At the group level, the mean beta weights corresponding to the models were tested against 0 (using one-sample *t* tests) and separate and combined models were tested against each other (using paired-samples *t* tests) within each type of surprise. Multiple comparisons were corrected for three sets of 640 *t* tests via a FDR correction

(FDR-corrected, $p < .01$) procedure (FDR; Benjamini et al., 2006).

Second, we examined Bayesian Pearson correlations between the mean amplitudes of the P3 responses following each type of unexpected event (auditory, visual, and haptic) and the corresponding mean RT. The subject-average amplitudes were determined by finding the largest positive-going amplitude deflection in the trial-average (at electrodes FCz and Cz) during the time-window ranging from 150 to 500 msec after the unexpected event (or in the case of the visual P3, we modified this search range to 250–600 msec based on the characteristics of the response reported in Wessel and Huber).

Third, the SST was employed as a functional localizer to demonstrate that the surprise-related FC P3 response shares a common neural generator with the inhibition-related FC P3 response in the SST. To this end, the two data sets from the CMO and SST task were merged, and the preprocessing steps and the ICA detailed above were repeated anew on the merged data sets. The stop-related P3 IC was selected automatically using a two-step spatio-temporal selection procedure (Wessel & Ullsperger, 2011). First, components were identified whose back-projected channel-space topography showed a maximum positive difference in stop compared with go trials in a FC ROI (consisting of electrodes FC1, FCz, FC2, C1, Cz, and C2 from among nine ROIs across the scalp). From these components, the component that showed the highest correlation to the original channel-space ERP in the same FC ROI and time window was selected for each participant as their stop-related IC. In Data Set 1, we validated the IC selected stop-signal P3 using a twofold procedure that addresses whether the stop-signal P3 occurs earlier on successful stops and whether its onset is positively correlated with SSRT. In short, we replicated prior work using this validation procedure (Wessel & Huber, 2019; Wessel & Aron, 2015; Kok et al., 2004). We do not report these results here (but refer the interested reader to the data and code on the Open Science Framework).

Fourth, we repeated the surprise model analyses detailed in (1) using only each participant's selected stop-related IC for the unexpected event in the CMO task. As control analyses, we subjected two other versions of the merged data set to the same analyses. These included reconstructions of the channel-space based on a back-projection of all original ICs *sans* the stop-related IC and a back-projection of the IC that accounted for the most residual variance after the stop-related IC was removed. As in (1), these tests were FDR-corrected for multiple comparisons (which again included 640 tests per set).

Replication of Wessel and Huber (2019) and Extension to Haptic Domain

We now report on the four results that we considered to be of primary importance (as detailed in the previous section) to replicate Wessel and Huber (2019) and extend their findings to the haptic domain.

First, using Data Set 1, we aimed to replicate the Wessel and Huber (2019) finding involving Bayesian surprise that a model with separate surprise terms for each modality would better explain the single-trial EEG response than the combined data and that the spatiotemporal dynamics of any significant time periods would relate to those of the P3 response. These tests were FDR-corrected for a family-wise alpha level of .01. As can be seen in Figure A1, the separate surprise term model showed a significant, positive prediction of the EEG data beginning with the 326- to 374-msec bin and extending through the remaining time bins (i.e., to 476–524 msec) to around the onset of the imperative stimulus. For the combined surprise term model, the 326- to 374-msec bin also showed a significant positive prediction of the EEG data, which also extended through the end of the trial. However, the separate surprise term model fit the data better than the combined surprise term model beginning with the 326- to 374-msec bin and onward. Compared with Wessel and Huber, the bin in which we first observed the separate surprise term model was slightly later (326–374 msec compared with 276–324 msec). This might be attributable to the larger sample size in Data Set 2 or the inclusion of unexpected events in the haptic modality in Data Set 1. Nevertheless, this time range coincided with the FC P3 response within each modality. In addition, the mean standardized beta weights at model-fitting electrodes identified by Wessel and Huber (FC2, C1, Cz, and C2) were all reliably above zero when fitting the Bayesian surprise model with separate modality terms. We therefore replicated Wessel and Huber with the current, trimodal data set in showing that a model with separate surprise terms (involving Bayesian surprise) predicts the single-trial EEG data.

Given that we examined β-bursts with respect to Shannon surprise (in addition to Bayesian surprise), we repeated the above analyses using Shannon surprise and with both data sets (because Wessel and Huber had not examined this for Data Set 2). For Data Set 1 (see Figure A1B), Shannon surprise fitted the whole-brain EEG data at some electrode sites (both positively and negatively), but rather inconsistently and not at FC sites. For Data Set 2, however, Shannon surprise significantly fit the data in the 326- to 374-msec time bin and at FC sites. Significant model fits were not found with common surprise terms, and no differences between model fits were found, either.

Second, we correlated the mean amplitude of the FC P3 response in each modality with mean RT (see Figure A2). Medium-sized positive correlations were found between RT and P3 amplitude following unexpected events in each modality, including the new haptic modality (unexpected visual: $r = .39$, $BF_{10} = 8.18$; unexpected audio: $r = .37$, $BF_{10} = 5.35$; unexpected haptic: $r = .32$, $BF_{10} = 2.45$). This is consistent with Wessel and Huber's findings in the auditory and visual modalities and further links this functional

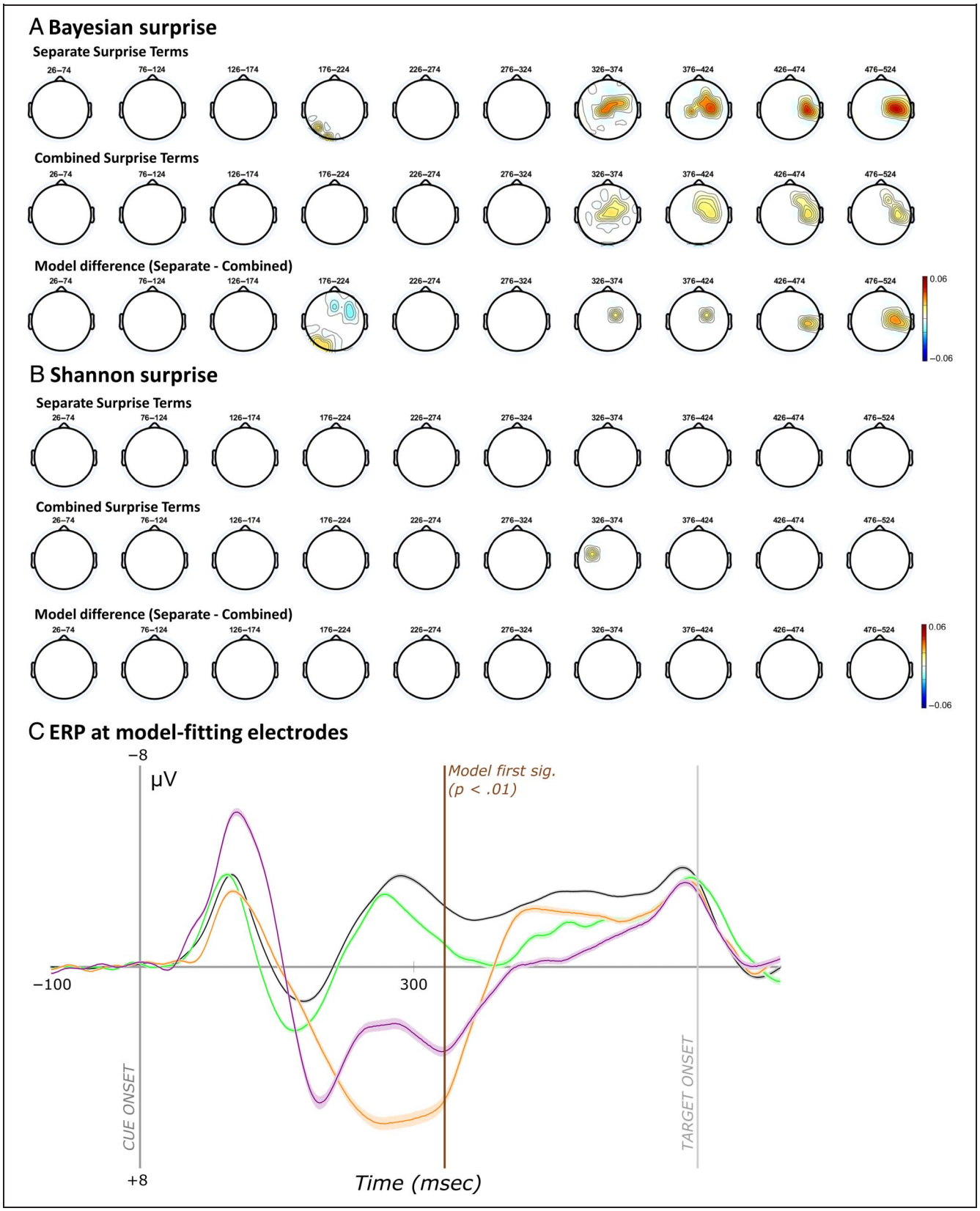

Figure A1. Scalp-topographies from modeling whole-brain single-trial EEG data with surprise and ERP at model-fitting electrodes in Data Set 1. (A) Topographies represent the mean standardized individual beta weights for Bayesian surprise and separate modality terms (top row), Bayesian surprise and combined modality terms (middle row), and the difference in fits between these two models (bottom row). Heatmaps reflect beta weights. (B) The same analyses as A but with Shannon surprise terms. (C) Cue-locked ERPs following each event type at model-fitting electrodes (FC2, C1, Cz, and C2) that were significant for the winning Bayesian surprise model and in Data Set 2. The spatiotemporal dynamics of the model-fitting electrodes correspond to the FC P3.

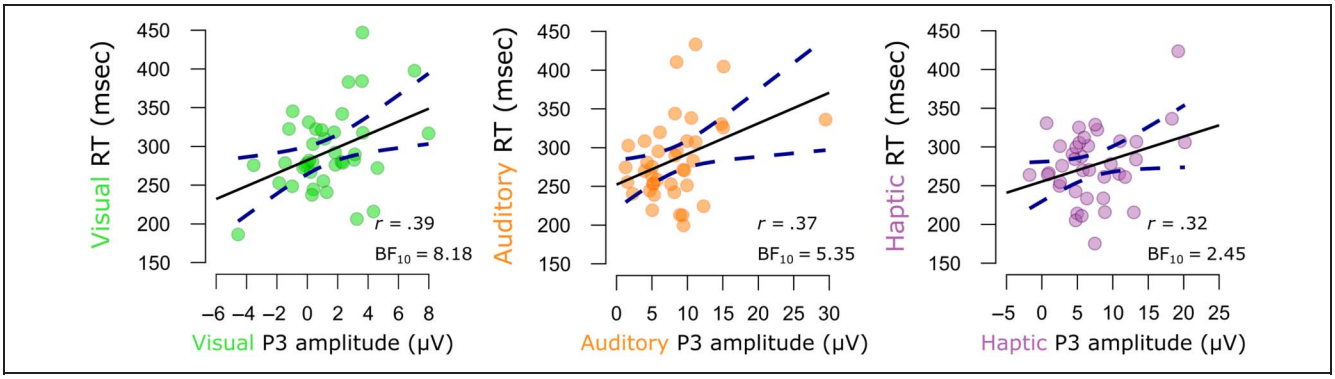

Figure A2. Pearson correlations between mean FC P3 amplitude and mean RTs following each type of unexpected event in Data Set 1. Dots indicate the means from individual participants. Solid black lines indicate the slope of the linear model. Dotted dark blue lines indicate the ±95% confidence intervals.

signature to inhibition (as larger responses brought about slower RTs).

Third, having merged the data sets from the visual SST and CMO tasks and having isolated a FC stop-related IC from each participant, we aimed to recover the FC P3 response using this one independent component. Because ICA serves to unmix a signal into its constituent (orthogonal) sources, identifying the FC P3 in the CMO

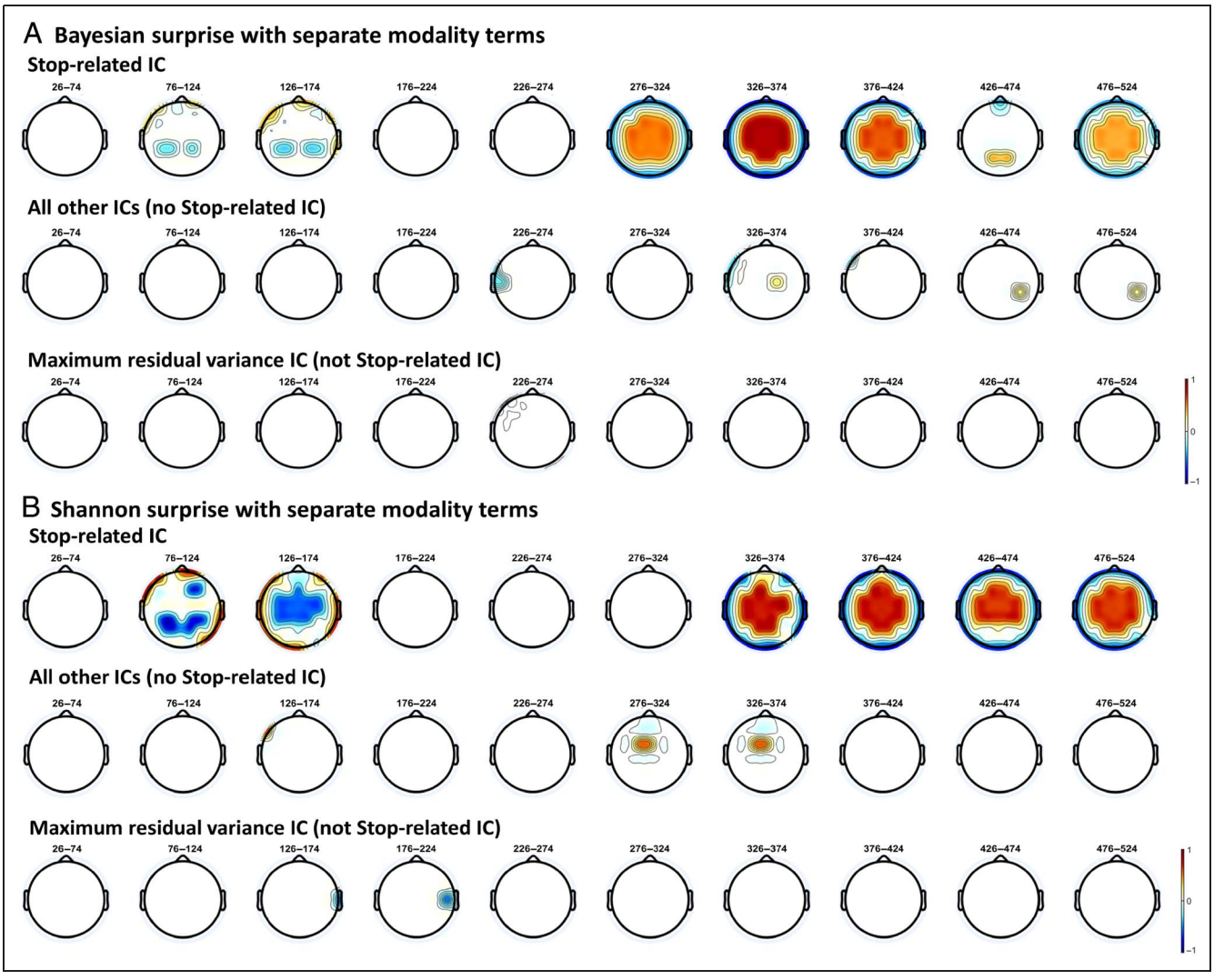

Figure A3. Scalp topographies of the ICs modeled with Bayesian surprise and Shannon surprise in the CMO task of Data Set 1 (n = 39). (A) Beta weights from the single-trial model-fitting of IC-EEG data with Bayesian surprise under the winning separate modality term model. Colors indicate significant model fits (warm colors = positive, cool colors = negative; white = nonsignificant, p = .01, FDR-corrected). (B) The same analyses but with Shannon surprise.

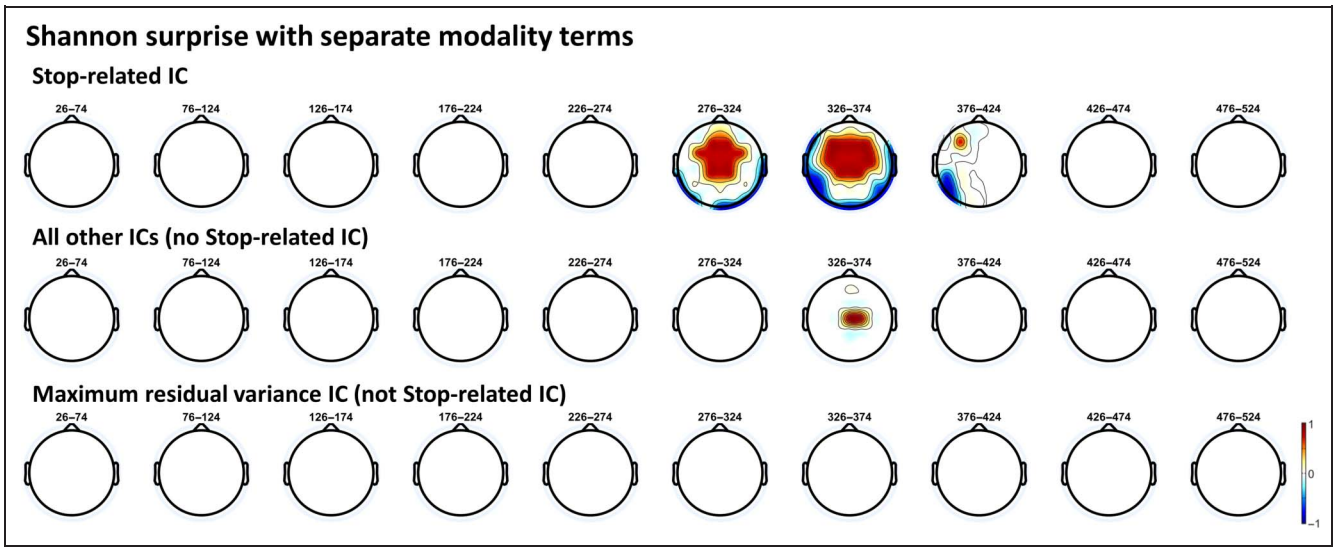

Figure A4. Scalp-topographies of the ICs modeled with Shannon surprise in the CMO task of Data Set 2 (n = 55). The same as Figure A3B but with Data Set 2.

task by using the SST as a functional localizer would suggest that a common neural generator is responsible for the FC P3 in both contexts. Because the SST was completed only in the visual modality, identification of FC P3 in the other auditory and haptic modalities would further highlight this signature as a domain-general inhibitory signature—granted, one that still retains information about the sensory modalities prompting inhibition (otherwise, the surprise model fitting results would have favored the common surprise term model). The difference waves are shown in Figure 8 in the main text. We were indeed able to produce the FC P3 in the CMO task when using the SST as a functional localizer task.

As our final replication of Wessel and Huber with Data Set 1, we repeated the above-mentioned whole-brain, single-trial EEG response modeling with surprise, this time using only the stop-related IC. For control analyses, we also completed these analyses using all other ICs and the IC that explained the most variance upon removal of the stop-related IC. As can be seen in Figure A3A, Bayesian surprise clearly fit the stop-related IC in Data Set 1. Moreover, this occurred at FC sites and timepoints consistent with the FC P3, suggesting that the neural generator involved in action inhibition in the SST also tracked surprise within the context of the CMO task. Interestingly, with the stop-related IC, Shannon surprise also fit the data at similar electrode sites and timepoints (although Shannon surprise became significant at FC sites in the 326–374 msec as opposed to the 276–324 msec, which was significant with Bayesian surprise). This contrasts the model-fitting analysis involving the full EEG data, which did not show this relationship to Shannon surprise (see Figure A1). Data Set 2 also replicated this finding of positive relationships between Shannon surprise and stop-related IC activity at FC sites. Here, significant model fits were found in the 276- to 324- and 326- to 374-msec bins. Most basically, the results from the IC-based approach replicate Data Set 2 in suggesting that the FC P3 process involved in action stopping also tracks surprise within the context of a CMO task. We further show here that using the IC-based approach, Shannon surprise also predicts activity at FC sites around the time of the FC P3 in Data Set 2 (see Figure A4). This could simply be because our experimental designs did not attempt to decorrelate Bayesian surprise and Shannon surprise. Future work might attempt to do so by intentionally introducing long stretches of intervening standard events between the same type of unexpected events to see if FC P3 is better captured by Bayesian surprise and whether another IC relating to the centroparietal P3 better captures Shannon surprise (e.g., Seer et al., 2016; Mars et al., 2008).

Acknowledgments

We thank Saara Engineer, Nathan Chalkley, Nathan Chen, and Kylie Dolan for their help with data collection. We thank Benjamin Rangel for assistance with the setup and monitoring of the startle response in pilot participants before and after experimentation. We thank two anonymous reviewers for suggesting additional supporting analyses.

Reprint requests should be sent to Joshua R. Tatz, Department of Psychological and Brain Sciences, University of Iowa, 340 Iowa Ave., Iowa City, IA, 52242, or via e-mail: Joshua-tatz@uiowa.edu.

Data Availability Statement

Data, scripts, and task code are available on the Open Science Framework at https://osf.io/nwkhf.

Author Contributions

Joshua R. Tatz: Conceptualization; Formal analysis; Investigation; Visualization; Writing—Original Draft, Writing—

Review & editing. Alec Mather: Conceptualization; Formal analysis; Investigation. Jan R. Wessel: Conceptualization; Formal analysis; Funding acquisition; Investigation; Project administration; Supervision; Writing—Review & editing.

Funding Information

Jan R. Wessel, National Institute of Neurological Disorders and Stroke (https://dx.doi.org/10.13039/100000065), grant number: R01 NS102201. Jan R. Wessel, National Institute of Neurological Disorders and Stroke (https://dx.doi.org/10.13039/100000065), grant number: R01 NS117753.

Diversity in Citation Practices

Retrospective analysis of the citations in every article published in this journal from 2010 to 2021 reveals a persistent pattern of gender imbalance: Although the proportions of authorship teams (categorized by estimated gender identification of first author/last author) publishing in the *Journal of Cognitive Neuroscience* (*JoCN*) during this period were M(an)/M = .407, W(oman)/M = .32, M/W = .115, and W/W = .159, the comparable proportions for the articles that these authorship teams cited were M/M = .549, W/M = .257, M/W = .109, and W/W = .085 (Postle and Fulvio, *JoCN*, 34:1, pp. 1–3). Consequently, *JoCN* encourages all authors to consider gender balance explicitly when selecting which articles to cite and gives them the opportunity to report their article's gender citation balance. The authors of this article report its proportions of citations by gender category to be as follows: M/M = .7, W/M = .22, M/W = .04, and W/W = .04.

Note

1. We note that using a similar procedure to identifying onsets on the β-burst data returned earlier differences than the peak in only a handful of participants; we therefore only considered peak burst latency in the ensuing analyses.

REFERENCES

Anidi, C., O'Day, J. J., Anderson, R. W., Afzal, M. F., Syrkin-Nikolau, J., Velisar, A., et al. (2018). Neuromodulation targets pathological not physiological beta bursts during gait in Parkinson's disease. *Neurobiology of Disease*, *120*, 107–117. https://doi.org/10.1016/j.nbd.2018.09.004, PubMed: 30196050

Aron, A. R. (2011). From reactive to proactive and selective control: Developing a richer model for stopping inappropriate responses. *Biological Psychiatry*, *69*, E55–E68. https://doi.org/10.1016/j.biopsych.2010.07.024, PubMed: 20932513

Asplund, C. L., Todd, J. J., Snyder, A. P., Gilbert, C. M., & Marois, R. (2010). Surprise-induced blindness: A stimulus-driven attentional limit to conscious perception. *Journal of Experimental Psychology: Human Perception and Performance*, *36*, 1372–1381. https://doi.org/10.1037/a0020551, PubMed: 20919779

Badry, R., Mima, T., Aso, T., Nakatsuka, M., Abe, M., Fathi, D., et al. (2009). Suppression of human cortico-motoneuronal excitability during the stop-signal task. *Clinical Neurophysiology*, *120*, 1717–1723. https://doi.org/10.1016/j.clinph.2009.06.027, PubMed: 19683959

Baker, S. N. (2007). Oscillatory interactions between sensorimotor cortex and the periphery. *Current Opinion in Neurobiology*, *17*, 649–655. https://doi.org/10.1016/j.conb.2008.01.007, PubMed: 18339546

Baldi, P., & Itti, L. (2010). Of bits and wows: A Bayesian theory of surprise with applications to attention. *Neural Networks*, *23*, 649–666. https://doi.org/10.1016/j.neunet.2009.12.007, PubMed: 20080025

Bell, A. J., & Sejnowski, T. J. (1995). An information-maximization approach to blind separation and blind deconvolution. *Neural Computation*, *7*, 1129–1159. https://doi.org/10.1162/neco.1995.7.6.1129, PubMed: 7584893

Benjamini, Y., Krieger, A. M., & Yekutieli, D. (2006). Adaptive linear step-up procedures that control the false discovery rate. *Biometrika*, *93*, 491–507. https://doi.org/10.1093/biomet/93.3.491

Boehler, C. N., Schevernels, H., Hopf, J.-M., Stoppel, C. M., & Krebs, R. M. (2014). Reward prospect rapidly speeds up response inhibition via reactive control. *Cognitive, Affective, & Behavioral Neuroscience*, *14*, 593–609. https://doi.org/10.3758/s13415-014-0251-5, PubMed: 24448735

Brainard, D. H. (1997). The Psychophysics Toolbox. *Spatial Vision*, *10*, 433–436. https://doi.org/10.1163/156856897X00357, PubMed: 9176952

Cai, W., Oldenkamp, C. L., & Aron, A. R. (2012). Stopping speech suppresses the task-irrelevant hand. *Brain and Language*, *120*, 412–415. https://doi.org/10.1016/j.bandl.2011.11.006, PubMed: 22206872

Chikazoe, J., Jimura, K., Hirose, S., Yamashita, K., Miyashita, Y., & Konishi, S. (2009). Preparation to inhibit a response complements response inhibition during performance of a stop-signal task. *Journal of Neuroscience*, *29*, 15870–15877. https://doi.org/10.1523/JNEUROSCI.3645-09.2009, PubMed: 20016103

Choo, Y., Matzke, D., Bowren, M. D., Tranel, D., & Wessel, J. R. (2022). Right inferior frontal cortex damage impairs the initiation of inhibitory control, but not its implementation. *eLife*, *11*, e79667. https://doi.org/10.7554/eLife.79667, PubMed: 36583378

Corbetta, M., & Shulman, G. L. (2002). Control of goal-directed and stimulus-driven attention in the brain. *Nature Reviews Neuroscience*, *3*, 201–215. https://doi.org/10.1038/nrn755, PubMed: 11994752

Delorme, A., & Makeig, S. (2004). EEGLAB: An open source toolbox for analysis of single-trial EEG dynamics including independent component analysis. *Journal of Neuroscience Methods*, *134*, 9–21. https://doi.org/10.1016/j.jneumeth.2003.10.009, PubMed: 15102499

Delorme, A., Palmer, J., Onton, J., Oostenveld, R., & Makeig, S. (2012). Independent EEG sources are dipolar. *PLoS One*, *7*, e30135. https://doi.org/10.1371/journal.pone.0030135, PubMed: 22355308

Delorme, A., Sejnowski, T., & Makeig, S. (2007). Enhanced detection of artifacts in EEG data using higher-order statistics and independent component analysis. *Neuroimage*, *34*, 1443–1449. https://doi.org/10.1016/j.neuroimage.2006.11.004, PubMed: 17188898

Diesburg, D. A., Greenlee, J. D. W., & Wessel, J. R. (2021). Cortico-subcortical β burst dynamics underlying movement cancellation in humans. *eLife*, *10*, e70270. https://doi.org/10.7554/eLife.70270, PubMed: 34874267

Diesburg, D. A., & Wessel, J. R. (2021). The pause-then-cancel model of human action-stopping: Theoretical considerations and empirical evidence. *Neuroscience & Biobehavioral*

Reviews, *129*, 17–34. https://doi.org/10.1016/j.neubiorev.2021.07.019, PubMed: 34293402

Duque, J., Greenhouse, I., Labruna, L., & Ivry, R. B. (2017). Physiological markers of motor inhibition during human behavior. *Trends in Neurosciences*, *40*, 219–236. https://doi.org/10.1016/j.tins.2017.02.006, PubMed: 28341235

Dutra, I. C., Waller, D. A., & Wessel, J. R. (2018). Perceptual surprise improves action stopping by nonselectively suppressing motor activity via a neural mechanism for motor inhibition. *Journal of Neuroscience*, *38*, 1482–1492. https://doi.org/10.1523/JNEUROSCI.3091-17.2017, PubMed: 29305533

Egner, T., Monti, J. M., & Summerfield, C. (2010). Expectation and surprise determine neural population responses in the ventral visual stream. *Journal of Neuroscience*, *30*, 16601–16608. https://doi.org/10.1523/JNEUROSCI.2770-10.2010, PubMed: 21147999

Elchlepp, H., Lavric, A., Chambers, C. D., & Verbruggen, F. (2016). Proactive inhibitory control: A general biasing account. *Cognitive Psychology*, *86*, 27–61. https://doi.org/10.1016/j.cogpsych.2016.01.004, PubMed: 26859519

Enz, N., Ruddy, K. L., Rueda-Delgado, L. M., & Whelan, R. (2021). Volume of β-bursts, but not their rate, predicts successful response inhibition. *Journal of Neuroscience*, *41*, 5069–5079. https://doi.org/10.1523/JNEUROSCI.2231-20.2021, PubMed: 33926997

Feingold, J., Gibson, D. J., DePasquale, B., & Graybiel, A. M. (2015). Bursts of beta oscillation differentiate postperformance activity in the striatum and motor cortex of monkeys performing movement tasks. *Proceedings of the National Academy of Sciences, U.S.A.*, *112*, 13687–13692. https://doi.org/10.1073/pnas.1517629112, PubMed: 26460033

Fischer, A. G., & Ullsperger, M. (2013). Real and fictive outcomes are processed differently but converge on a common adaptive mechanism. *Neuron*, *79*, 1243–1255. https://doi.org/10.1016/j.neuron.2013.07.006, PubMed: 24050408

Friston, K. (2010). The free-energy principle: A unified brain theory? *Nature Reviews Neuroscience*, *11*, 127–138. https://doi.org/10.1038/nrn2787, PubMed: 20068583

Hakim, N., Feldmann-Wustefeld, T., Awh, E., & Vogel, E. K. (2021). Controlling the flow of distracting information in working memory. *Cerebral Cortex*, *31*, 3323–3337. https://doi.org/10.1093/cercor/bhab013, PubMed: 33675357

Horstmann, G. (2015). The surprise-attention link: A review. *Annals of the New York Academy of Sciences*, *1339*, 106–115. https://doi.org/10.1111/nyas.12679, PubMed: 25682693

Iacullo, C., Diesburg, D. A., & Wessel, J. R. (2020). Non-selective inhibition of the motor system following unexpected and expected infrequent events. *Experimental Brain Research*, *238*, 2701–2710. https://doi.org/10.1007/s00221-020-05919-3, PubMed: 32948892

Jahfari, S., Stinear, C. M., Claffey, M., Verbruggen, F., & Aron, A. R. (2010). Responding with restraint: What are the neurocognitive mechanisms? *Journal of Cognitive Neuroscience*, *22*, 1479–1492. https://doi.org/10.1162/jocn.2009.21307, PubMed: 19583473

Jana, S., Hannah, R., Muralidharan, V., & Aron, A. R. (2020). Temporal cascade of frontal, motor and muscle processes underlying human action-stopping. *eLife*, *9*, e50371. https://doi.org/10.7554/eLife.50371, PubMed: 32186515

Kim, H. (2014). Involvement of the dorsal and ventral attention networks in oddball stimulus processing: A meta-analysis. *Human Brain Mapping*, *35*, 2265–2284. https://doi.org/10.1002/hbm.22326, PubMed: 23900833

Kok, A., Ramautar, J. R., De Ruiter, M. B., Band, G. P. H., & Ridderinkhof, K. R. (2004). ERP components associated with successful and unsuccessful stopping in a stop-signal task. *Psychophysiology*, *41*, 9–20. https://doi.org/10.1046/j.1469-8986.2003.00127.x, PubMed: 14692996

Kolossa, A., Kopp, B., & Fingscheidt, T. (2015). A computational analysis of the neural bases of Bayesian inference. *Neuroimage*, *106*, 222–237. https://doi.org/10.1016/j.neuroimage.2014.11.007, PubMed: 25462794

Law, R. G., Pugliese, S., Shin, H., Sliva, D. D., Lee, S., Neymotin, S., et al. (2022). Thalamocortical mechanisms regulating the relationship between transient beta events and human tactile perception. *Cerebral Cortex*, *32*, 668–688. https://doi.org/10.1093/cercor/bhab221, PubMed: 34401898

Lee, T. W., Girolami, M., & Sejnowski, T. J. (1999). Independent component analysis using an extended infomax algorithm for mixed subgaussian and supergaussian sources. *Neural Computation*, *11*, 417–441. https://doi.org/10.1162/089976699300016719, PubMed: 9950738

Levy, B. J., & Wagner, A. D. (2011). Cognitive control and right ventrolateral prefrontal cortex: Reflexive reorienting, motor inhibition, and action updating. *Annals of the New York Academy of Sciences*, *1224*, 40–62. https://doi.org/10.1111/j.1749-6632.2011.05958.x, PubMed: 21486295

Little, S., Bonaiuto, J., Barnes, G., & Bestmann, S. (2019). Human motor cortical beta bursts relate to movement planning and response errors. *PLoS Biology*, *17*, e3000479. https://doi.org/10.1371/journal.pbio.3000479, PubMed: 31584933

Lofredi, R., Tan, H., Neumann, W.-J., Yeh, C.-H., Schneider, G.-H., Kühn, A. A., et al. (2019). Beta bursts during continuous movements accompany the velocity decrement in Parkinson's disease patients. *Neurobiology of Disease*, *127*, 462–471. https://doi.org/10.1016/j.nbd.2019.03.013, PubMed: 30898668

Love, J., Selker, R., Marsman, M., Jamil, T., Dropmann, D., Verhagen, J., et al. (2019). JASP: Graphical statistical software for common statistical designs. *Journal of Statistical Software*, *88*, 1–17. https://doi.org/10.18637/jss.v088.i02

Mars, R. B., Debener, S., Gladwin, T. E., Harrison, L. M., Haggard, P., Rothwell, J. C., et al. (2008). Trial-by-trial fluctuations in the event-related electroencephalogram reflect dynamic changes in the degree of surprise. *Journal of Neuroscience*, *28*, 12539–12545. https://doi.org/10.1523/JNEUROSCI.2925-08.2008, PubMed: 19020046

Muralidharan, V., Aron, A. R., & Schmidt, R. (2022). Transient beta modulates decision thresholds during human action-stopping. *Neuroimage*, *254*, 119145. https://doi.org/10.1016/j.neuroimage.2022.119145, PubMed: 35342005

Nassar, M. R., Bruckner, R., & Frank, M. J. (2019). Statistical context dictates the relationship between feedback-related EEG signals and learning. *eLife*, *8*, e46975. https://doi.org/10.7554/eLife.46975, PubMed: 31433294

Novembre, G., Pawar, V. M., Bufacchi, R. J., Kilintari, M., Srinivasan, M., Rothwell, J. C., et al. (2018). Saliency detection as a reactive process: Unexpected sensory events evoke corticomuscular coupling. *Journal of Neuroscience*, *38*, 2385–2397. https://doi.org/10.1523/JNEUROSCI.2474-17.2017, PubMed: 29378865

O'Reilly, J. X., Schuffelgen, U., Cuell, S. F., Behrens, T. E., Mars, R. B., & Rushworth, M. F. (2013). Dissociable effects of surprise and model update in parietal and anterior cingulate cortex. *Proceedings of the National Academy of Sciences, U.S.A.*, *110*, E3660–E3669. https://doi.org/10.1073/pnas.1305373110, PubMed: 23986499

Parmentier, F. B. R., Elford, G., Escera, C., Andrés, P., & San Miguel, I. (2008). The cognitive locus of distraction by acoustic novelty in the cross-modal oddball task. *Cognition*, *106*, 408–432. https://doi.org/10.1016/j.cognition.2007.03.008, PubMed: 17445791

Perrin, F., Pernier, J., Bertrand, O., & Echallier, J. F. (1989). Spherical splines for scalp potential and current density mapping. *Electroencephalography and Clinical Neurophysiology*, *72*, 184–187. https://doi.org/10.1016/0013-4694(89)90180-6, PubMed: 2464490

Phillips, H. N., Blenkmann, A., Hughes, L. E., Kochen, S., Bekinschtein, T. A., Cam, C., et al. (2016). Convergent evidence for hierarchical prediction networks from human electrocorticography and magnetoencephalography. *Cortex*, *82*, 192–205. https://doi.org/10.1016/j.cortex.2016.05.001, PubMed: 27389803

Piña-Fuentes, D., van Zijl, J. C., van Dijk, J. M. C., Little, S., Tinkhauser, G., Oterdoom, D. L. M., et al. (2019). The characteristics of pallidal low-frequency and beta bursts could help implementing adaptive brain stimulation in the Parkinsonian and dystonic internal globus pallidus. *Neurobiology of Disease*, *121*, 47–57. https://doi.org/10.1016/j.nbd.2018.09.014, PubMed: 30227227

Raud, L., & Huster, R. J. (2017). The temporal dynamics of response inhibition and their modulation by cognitive control. *Brain Topography*, *30*, 486–501. https://doi.org/10.1007/s10548-017-0566-y, PubMed: 28456867

Raud, L., Huster, R. J., Ivry, R. B., Labruna, L., Messel, M. S., & Greenhouse, I. (2020). A single mechanism for global and selective response inhibition under the influence of motor preparation. *Journal of Neuroscience*, *40*, 7921–7935. https://doi.org/10.1523/JNEUROSCI.0607-20.2020, PubMed: 32928884

Schmidt, R., & Berke, J. D. (2017). A pause-then-cancel model of stopping: Evidence from basal ganglia neurophysiology. *Philosophical Transactions of the Royal Society of London, Series B: Biological Sciences*, *372*, 20160202. https://doi.org/10.1098/rstb.2016.0202, PubMed: 28242736

Sebastian, A., Konken, A. M., Schaum, M., Lieb, K., Tüscher, O., & Jung, P. (2021). Surprise: Unexpected action execution and unexpected inhibition recruit the same fronto-basal-ganglia network. *Journal of Neuroscience*, *41*, 2447–2456. https://doi.org/10.1523/JNEUROSCI.1681-20.2020, PubMed: 33376157

Seer, C., Lange, F., Boos, M., Dengler, R., & Kopp, B. (2016). Prior probabilities modulate cortical surprise responses: A study of event-related potentials. *Brain and Cognition*, *106*, 78–89. https://doi.org/10.1016/j.bandc.2016.04.011, PubMed: 27266394

Shannon, C. E. (1948). A mathematical theory of communication. *Bell System Technical Journal*, *27*, 379–423. https://doi.org/10.1002/j.1538-7305.1948.tb01338.x

Sherman, M. A., Lee, S., Law, R., Haegens, S., Thorn, C. A., Hämäläinen, M. S., et al. (2016). Neural mechanisms of transient neocortical beta rhythms: Converging evidence from humans, computational modeling, monkeys, and mice. *Proceedings of the National Academy of Sciences, U.S.A.*, *113*, E4885–E4894. https://doi.org/10.1073/pnas.1604135113, PubMed: 27469163

Shin, H., Law, R., Tsutsui, S., Moore, C. I., & Jones, S. R. (2017). The rate of transient beta frequency events predicts behavior across tasks and species. *eLife*, *6*, e29086. https://doi.org/10.7554/eLife.29086, PubMed: 29106374

Soh, C., Hynd, M., Rangel, B. O., & Wessel, J. R. (2021). Adjustments to proactive motor inhibition without effector-specific foreknowledge are reflected in a bilateral upregulation of sensorimotor beta-burst rates. *Journal of Cognitive Neuroscience*, *33*, 784–798. https://doi.org/10.1162/jocn_a_01682, PubMed: 34449841

Soh, C., & Wessel, J. R. (2021). Unexpected sounds nonselectively inhibit active visual stimulus representations. *Cerebral Cortex*, *31*, 1632–1646. https://doi.org/10.1093/cercor/bhaa315, PubMed: 33140100

Tatz, J. R., Soh, C., & Wessel, J. R. (2021). Common and unique inhibitory control signatures of action-stopping and attentional capture suggest that actions are stopped in two stages. *Journal of Neuroscience*, *41*, 8826–8838. https://doi.org/10.1523/JNEUROSCI.1105-21.2021, PubMed: 34493541

Tenke, C. E., & Kayser, J. (2005). Reference-free quantification of EEG spectra: Combining current source density (CSD) and frequency principal components analysis (fPCA). *Clinical Neurophysiology*, *116*, 2826–2846. https://doi.org/10.1016/j.clinph.2005.08.007, PubMed: 16257577

Tinkhauser, G., Pogosyan, A., Little, S., Beudel, M., Herz, D. M., Tan, H., et al. (2017). The modulatory effect of adaptive deep brain stimulation on beta bursts in Parkinson's disease. *Brain*, *140*, 1053–1067. https://doi.org/10.1093/brain/awx010, PubMed: 28334851

Tinkhauser, G., Pogosyan, A., Tan, H., Herz, D. M., Kuhn, A. A., & Brown, P. (2017). Beta burst dynamics in Parkinson's disease OFF and ON dopaminergic medication. *Brain*, *140*, 2968–2981. https://doi.org/10.1093/brain/awx252, PubMed: 29053865

Tinkhauser, G., Torrecillos, F., Duclos, Y., Tan, H., Pogosyan, A., Fischer, P., et al. (2018). Beta burst coupling across the motor circuit in Parkinson's disease. *Neurobiology of Disease*, *117*, 217–225. https://doi.org/10.1016/j.nbd.2018.06.007, PubMed: 29909050

Verbruggen, F., Aron, A. R., Band, G. P. H., Beste, C., Bissett, P. G., Brockett, A. T., et al. (2019). A consensus guide to capturing the ability to inhibit actions and impulsive behaviors in the stop-signal task. *eLife*, *8*, e46323. https://doi.org/10.7554/eLife.46323, PubMed: 31033438

Verbruggen, F., & Logan, G. D. (2009). Models of response inhibition in the stop-signal and stop-change paradigms. *Neuroscience & Biobehavioral Reviews*, *33*, 647–661. https://doi.org/10.1016/j.neubiorev.2008.08.014, PubMed: 18822313

Wessel, J. R. (2018a). A neural mechanism for surprise-related interruptions of visuospatial working memory. *Cerebral Cortex*, *28*, 199–212. https://doi.org/10.1093/cercor/bhw367, PubMed: 27909006

Wessel, J. R. (2018b). Surprise: A more realistic framework for studying action stopping? *Trends in Cognitive Sciences*, *22*, 741–744. https://doi.org/10.1016/j.tics.2018.06.005, PubMed: 30122169

Wessel, J. R. (2020). β-bursts reveal the trial-to-trial dynamics of movement initiation and cancellation. *Journal of Neuroscience*, *40*, 411–423. https://doi.org/10.1523/JNEUROSCI.1887-19.2019, PubMed: 31748375

Wessel, J. R., & Aron, A. R. (2013). Unexpected events induce motor slowing via a brain mechanism for action-stopping with global suppressive effects. *Journal of Neuroscience*, *33*, 18481–18491. https://doi.org/10.1523/JNEUROSCI.3456-13.2013, PubMed: 24259571

Wessel, J. R., & Aron, A. R. (2015). It's not too late: The onset of the frontocentral P3 indexes successful response inhibition in the stop-signal paradigm. *Psychophysiology*, *52*, 472–480. https://doi.org/10.1111/psyp.12374, PubMed: 25348645

Wessel, J. R., & Aron, A. R. (2017). On the globality of motor suppression: Unexpected events and their influence on behavior and cognition. *Neuron*, *93*, 259–280. https://doi.org/10.1016/j.neuron.2016.12.013, PubMed: 28103476

Wessel, J. R., & Huber, D. E. (2019). Frontal cortex tracks surprise separately for different sensory modalities but engages a common inhibitory control mechanism. *PLoS Computational Biology*, *15*, e1006927. https://doi.org/10.1371/journal.pcbi.1006927, PubMed: 31356593

Wessel, J. R., Reynoso, H. S., & Aron, A. R. (2013). Saccade suppression exerts global effects on the motor system. *Journal of Neurophysiology*, *110*, 883–890. https://doi.org/10.1152/jn.00229.2013, PubMed: 23699058

Wessel, J. R., & Ullsperger, M. (2011). Selection of independent components representing event-related brain potentials: A data-driven approach for greater objectivity. *Neuroimage*, *54*, 2105–2115. https://doi.org/10.1016/j.neuroimage.2010.10.033, PubMed: 20965258